IEEE Access
Multidisciplinary ⋮ Rapid Review ⋮ Open Access Journal

Received 5 April 2023, accepted 30 April 2023, date of publication 9 May 2023, date of current version 19 May 2023.

Digital Object Identifier 10.1109/ACCESS.2023.3274684

RESEARCH ARTICLE

Performance Evaluation of Static PV Array Configurations for Mitigating Mismatch Losses

S. DEVAKIRUBAKARAN[1], RAJESH VERMA[2], BHARATIRAJA CHOKKALINGAM[1], (Senior Member, IEEE), AND LUCIAN MIHET-POPA[3], (Senior Member, IEEE)

[1]Center for Electric Mobility, Department of Electrical and Electronics Engineering, SRM Institute of Science and Technology, Kattankulathur, Tamil Nadu 603 203, India
[2]Department of Electrical Engineering, College of Engineering, King Khalid University, Abha, Asir 61411, Saudi Arabia
[3]Faculty of Information Technology, Engineering and Economics, Østfold University College, 1757 Halden, Norway

Corresponding authors: Bharatiraja Chokkalingam (bharatic@srmist.edu.in) and Lucian Mihet-Popa (lucian.mihet@hiof.no)

This work was supported in part by the Department of Science and Technology, Government of India, Promotion of University Research and Scientific Excellence (PURSE), under Award SR/PURSE/2021/65; and in part by the Deanship of Scientific Research, King Khalid University, through a Large Group Research Project, under Grant RGP 2/177/44.

ABSTRACT Solar photovoltaic (PV) systems are susceptible to power loss caused by environmental factors such as partial shading and temperature changes. To address this issue, PV modules are connected in array configurations. However, these configurations can lead to mismatch losses between the PV rows, which reduce power output. While there are many solutions to mitigate these losses, the performance of each solution can vary depending on the environmental conditions and the array configuration logic. This research paper evaluates the performance of fifteen existing static PV array configuration techniques under various shading patterns. We analyze the mathematical formulation and logic used behind each configuration, as well as the shade dispersion rate, power generation, power losses, advantages, and disadvantages. Our analysis includes a MATLAB/Simulink® model of a 5×5 array for each configuration under different shading patterns. The performance of consistent and best configurations is also evaluated in a real-time environment. The results categorize each configuration as consistent, best, average, or poor. This paper provides a detailed analysis of the different PV array configurations and their performance, which can help in selecting the optimal configuration for specific environmental conditions.

INDEX TERMS Mismatch losses, partial shading, PV array configuration, shade dispersion, shading patterns, static configurations.

I. INTRODUCTION

The most reliable energy source for future energy demand is solar energy [1], [2]. Solar thermal collectors and solar photovoltaic systems are two options for harvesting solar energy. In solar thermal collectors, the heat energy from the sun is utilized for energy generation, whereas, in solar photovoltaic systems solar irradiation is directly converted into electricity based on the photovoltaic effect [3]. The solar photovoltaic system is the most suitable one for residual installations as well as for rural electrification [4]. The solar PV system has many advantages over other renewable energy sources like wind, bio-mass, tidal, etc., Apart from its merits; it experiences some factors that reduce the overall performance of the PV system. The main factors behind the power losses are as follows, i) partial shading [5], [6], [7], [8], [9], [10], [11], [12], [13], [14], [15], ii) hotspot, iii) temperature [16], iv) delamination [17], [18], v) dust formation [19], [20], [21], etc., Regards the power loss causing factors, some of them like dust and dirt formation are limitable by proper maintenance, some of them like partial shading are resistible by proper arrangements, some of them are avoidable by the proper installation and some of the environmental factors cannot be controlled and avoided. The effects of dust and

The associate editor coordinating the review of this manuscript and approving it for publication was Xiaodong Liang.

dirt formation can be avoided by proper cleaning at regular intervals. But the occurrence of partial shading is not a predictable phenomenon, so it causes severe power loss in the system. The various factors cause the partial shading is given in Figure 1. The bypass diodes are used for the PV system for reducing the hotspots [22], [23], [24], [25], [26], [27], [28], [29], [30]. The current flow through the faulty cells increases the operating temperature which results in the hotspot. The PV cell with the hotspots is acting as a load and affecting the nearby healthy cells. The bypass diodes are connected across the PV cells so that the current flow through the faulty cells is avoided. However, the usage of a bypass diode causes many local maximum power points (LMPP) in the Power-Voltage (P-V) and Current-Voltage (I-V) curves, whereas, P-V and I-V characteristic curves are used to study the performance of the PV cell [9], [31], [32], [33]. Maximum Power Point Tracking (MPPT) is a technique used in PV converters for operating the PV system at the maximum power extraction point [34], [35], [36], [37], [38], [39], [40], [41], [42], [43], [44], [45]. The usage of bypass diodes in the PV system leads to power generation with more than one LMPP. This leads to the misidentification of Global Maximum Power Point (GMPP) among the various LMPPs. The accuracy of the conventional MPPT algorithms like Perturb & Observe (P&O) and Incremental Conductance (InC) algorithms is very less in finding the GMPP. So, the conventional MPPT algorithms are replaced with the use of optimization problems like Neural Networks, Artificial Neural Networks (ANN), Ant Colony Optimization (ACO), and Particle Swarm Optimization (PSO) for increasing the accuracy of the MPPT algorithms. However, the tacking of MPP is failed in most of the complex cases that result in power loss. The MPPT technique is not efficient at all times of power generation.

However, the evolution of PV array topologies creates the possibility of minimizing the effects of partial shading and other minor faults. Since a single cell or single module could not produce enough power to efficiently power the entire load, the PV modules are connected in specific structures like series or parallel to meet the load demand. As a result, the idea of a PV array arrangement emerged from grouping PV modules into a PV array to meet the energy requirement. Initially, these techniques were used for the bulk generation, but they gained more significance due to their enhanced power-extracting capability [46], [47], [48], [49], [50], [51], [52], [53], [54], [55], [56], [57], [58], [59], [60], [61], [62], [63], [64], [65], [66], [67], [68], [69], [70], [71], [72], [73], [74], [75], [76], [77], [78], [79], [80], [81]. Series (Se) and Series-Parallel (Se-P) array configurations are the conventional methods used earlier in the PV system. The basic concept behind this array configuration method is to supply the bulk power demand. However, the efficiency of these conventional methods is highly influenced by partial shading and other environmental factors. In basic, the current in the series connection and voltage in the parallel connection is the same as in the single source. At the same, the voltage in the series connection and current in the parallel connection are equal to the sum of the sources in the corresponding string

When the current sources are connected in the series connection, the current output at the load terminal is limited by the source with a minimum current rating. This same phenomenon is reflected in the series connection of PV modules. The PV modules with similar specifications are used for the array formation (i.e., array configuration). But the current generation of the PV array is affected by partial shading and other faults. i.e., the shaded PV modules are generating less current as compared with the other healthy panels. So, the current generation of the entire PV string is limited by faulty PV cells/modules. This also causes mismatch losses in the TCT array configuration. The mismatch loss can be stated as, the difference between the minimum and maximum power-generating rows. The mismatch loss in the PV array should be in the range of 1% to 2% and when it exceeds more than 2%, indicate abnormalities in the PV system. PV array configuration is the key that is used for reducing the mismatch loss between the PV rows. The conventional array configurations like Se and Se-P failed in some complex shading patterns. For enhancing the effectiveness of the conventional methods, new logic and mathematical formulations were incorporated. These array configurations have a high resistive ability to the shading, i.e., they can disperse the shading evenly over the PV array and reduce the mismatch losses. Some of PV array configurations are given in table 1.

TABLE 1. Specification of PV modules.

References	Configurations	Type	Array Size	Efficiency Improvement
[96]	Socio-inspired democratic political algorithm	Dynamic	10X10 15X15 20X20	21.47% 21.55% 20.98%
[97]	zero switch and sensorless reconfiguration	static	4X4	19.07%
[87]	Two-step module placement approach	Dynamic	4X4	12.25%
[98]	Hybrid red deer with moth flame optimization	Dynamic	9X9	19.230
[99]	Dragonfly-based dynamic reconfiguration	Dynamic	3X3 9X9	22%
[100]	Novel prime numbers-based PV array reconfiguration	Dynamic	9X9 23X23	8.77%
[101]	Electrical reconfiguration in partial shading-prone solar PV arrays	Dynamic	3X3	22.96%
[102]	MMTES algorithm	Dynamic	3X3	22.5%
[103]	Shade dispersion interconnection scheme	Dynamic	3X3 7X7	20.46%
[104]	Dynamic Mismatch Loss mitigation Algorithm	Dynamic	2X2	29%

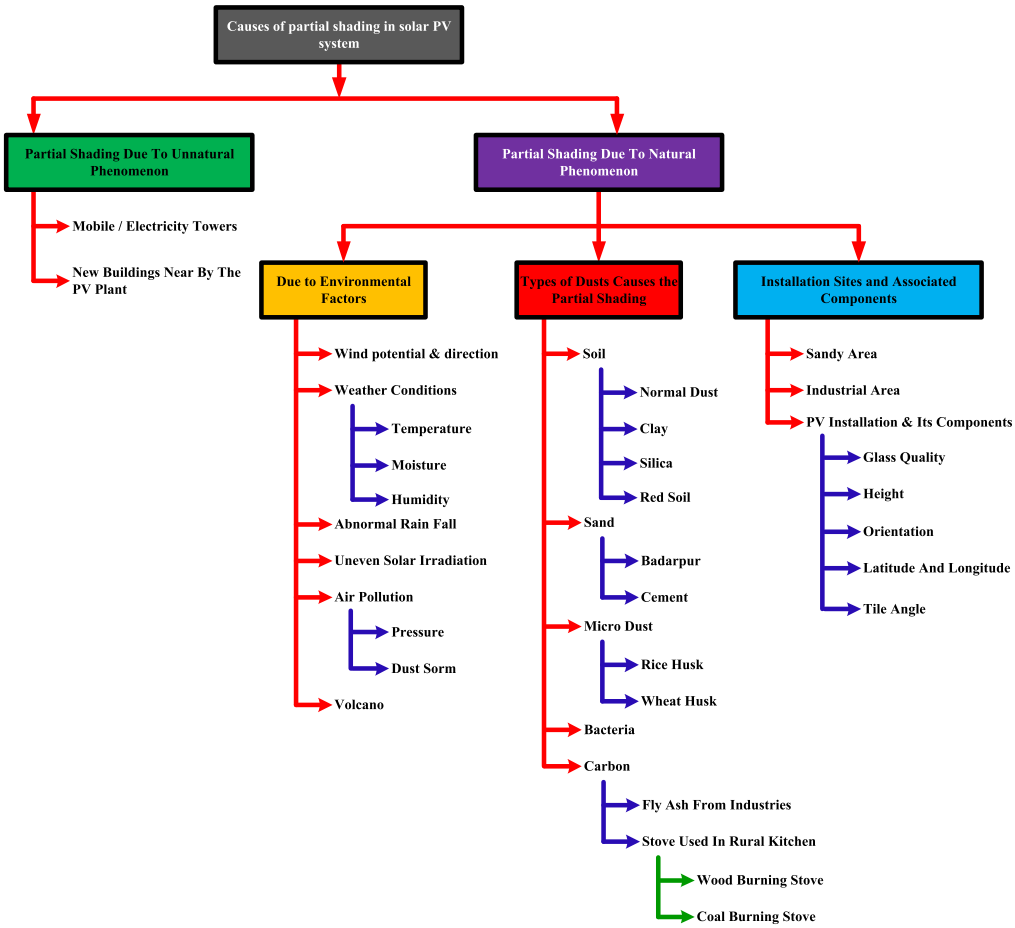

FIGURE 1. Causes of partial shading in the PV system.

The reconfiguration technique is another solution that has been developed for reducing the mismatch losses in the PV system. The sensors and switches are used to rearrange the electrical interconnection of the PV modules. In, [84], it proposes a two-step reconfiguration method to reduce mismatch losses between the PV rows. For reducing power losses, this reconfiguration technique works well in complex shading patterns. Other types of reconfiguration strategies were discussed in [85], [86], [87], and [88]. As compared to array configuration, the implementation and operating costs of reconfiguration methods are more expensive. The reconfiguration techniques also need regular maintenance. For identifying the PV cell defects, there are many approaches were proposed as in [89], [90], and [91]. These methods use electrical parameters, computational algorithms, Soft computing methods, image processing tools, and so on for obtaining the fault details in the PV system. The various array configuration techniques developed from the conventional methods are presented in this work. Also, these presented array configuration techniques are reviewed and validated in terms of performance, efficiency, the scope of practical implementation, and cost-effectiveness. Also, a detailed analysis of these configurations is presented in terms of efficiency, reliability, robustness, simplicity of implementation, the scope of the techniques, advantages, and disadvantages of each technique.

Following this introduction in section I, the mathematical modeling of the PV cell and array is described in section II, followed by a brief discussion of the various array configurations in section III, a performance analysis of the best configurations in a 5×5 PV array under various shading patterns in section IV, and a conclusion and the scope of the array configurations in section V

II. MATHEMATICAL MODELING OF PV CELL AND PV ARRAY

One of the factors determining the effectiveness of the PV system is the mathematical model of the PV cell. The PV system uses two different types of PV models, including the single-diode model [61] and the double-diode model [82], [83]. A current source, parallel-connected diode, and resistance were constructing an equivalent circuit for a PV cell. Figure 2 depicts the equivalent circuit for both the single and double-diode models. When compared to the single-diode model, the double-diode model produces more power with greater efficiency at low irradiation.

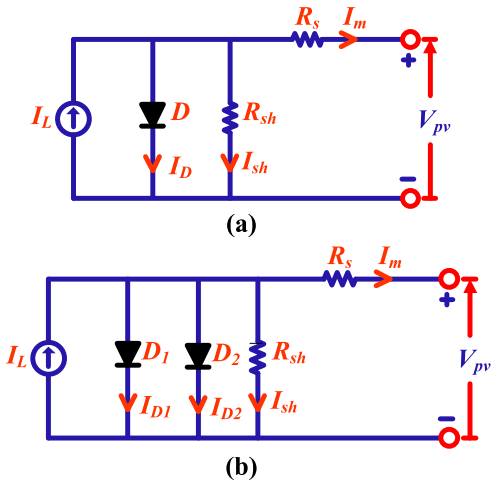

FIGURE 2. (a) Single diode model (b) Double diode model of PV cell.

The maximum current generated by the single-diode model of the PV cell can be expressed as (1)

$$I_m = I_L - I_D - I_{sh} \tag{1}$$

where, I_m is the maximum output current generated by the solar cell, and, I_L is the photo-generated current.

Equation (1) can be replaced with respect to voltage, number of cells in series, and resistance as equation (2)

$$I_m = I_L - I_{sat}\left[exp\left(\frac{V + IR_s}{nN_sV_{th}}\right) - 1\right] - \frac{V + IR_s}{R_{sh}} \tag{2}$$

The output current generated by the PV cell is directly proportional to the available solar irradiation and the temperature coefficient, whereas the current equation can be written in terms of solar irradiation and temperature as

$$I_{SC}(S,T) = (S_a/S_{STC})\left[I_{SC(STC)} + \mu_{ISC}(T_a - T_{STC})\right] \tag{3}$$

where I_{SC} is the rated short circuit current, S_a is the actual available solar irradiation, S_{STC} is the rated solar irradiance ($1000W/m^2$), Ta is the actual available temperature (°C), T_{STC} is the rated STC temperature (25°C), and μI_{sc} is the temperature coefficient of PV cell to the current.

The PV cell's voltage output highly depends on the PV cell temperature and positive temperature coefficient concerning the voltage. On other hand, the dependence of irradiation for voltage generation is the logarithmic function, and it does not make a high impact on the generation of voltage. The expression for the open circuit voltage can be derived as

$$V_{OC} = V_{OC(STC)} + \mu_{(V_{OC})}\left(T_a - T_{(STC)}\right) \tag{4}$$

where μ_{Voc} is the positive temperature coefficient of the PV cell concerning voltage. The voltage generation of the PV cell concerning the photocurrent, diode current, and resistances can be expressed as equation (5),

$$V_m = \frac{AkT_a}{e}\left(\frac{I_{ph} + I_D + I_m}{I_D}\right) - R_sI_m \tag{5}$$

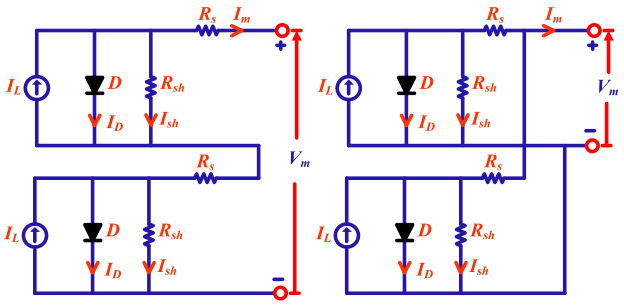

FIGURE 3. The electrical connection of PV cells (a) series (b) parallel.

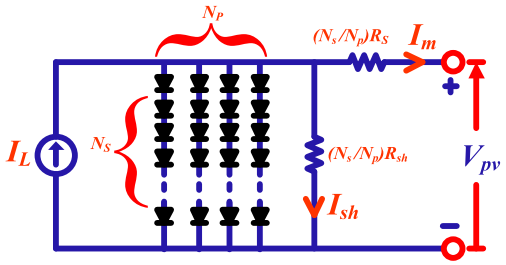

FIGURE 4. Schematic diagram of series-parallel PV array.

The voltage equation for the two-diode model PV cell is expressed as in equation (6)

$$V_m = \frac{AkT_a}{e}\left(\frac{I_{ph} + I_D - I_m}{I_D}\right) - I_m\left(\frac{R_sR_{sh}}{R_s + R_{sh}}\right) \tag{6}$$

where V_m is the maximum output voltage of the PV cell, I_D is the current flow through the diode, I_m is the maximum output current generated by the solar cell, R_s is the series resistance, and R_{sh} is the shunt resistance.

The power output of the solar cell can be represented as,

$$P_m = I_m \times V_m \tag{7}$$

The relation between the maximum voltage, the maximum current, and open-circuit voltage, short circuit current can derive as the fill factor as expressed in equation (8) as,

$$FillFactor, (FF) = \frac{Vm \times I_m}{V_{OC} \times I_{SC}} \tag{8}$$

Equation (6) can be modified by equation (7) as,

$$P_m = (V_{OC} \times I_{SC}) \times FillFactor \tag{9}$$

These are the basic mathematical equations used for modeling the PV array. The PV array integration is formed by connecting the PV cells in series and parallel as per the voltage and current requirement. The series and parallel connection of the PV array is shown in Figure 3. The schematic diagram of the PV array for the 'n' number of cells in series and the 'n' number of cells in parallel is shown in Figure 4. The number of cells connected in series is represented as N_s and the number of strings connected in parallel is represented as N_p.

The occurrence of partial shading is most dangerous to the PV system, which causes the hotspots in the PV cell surface

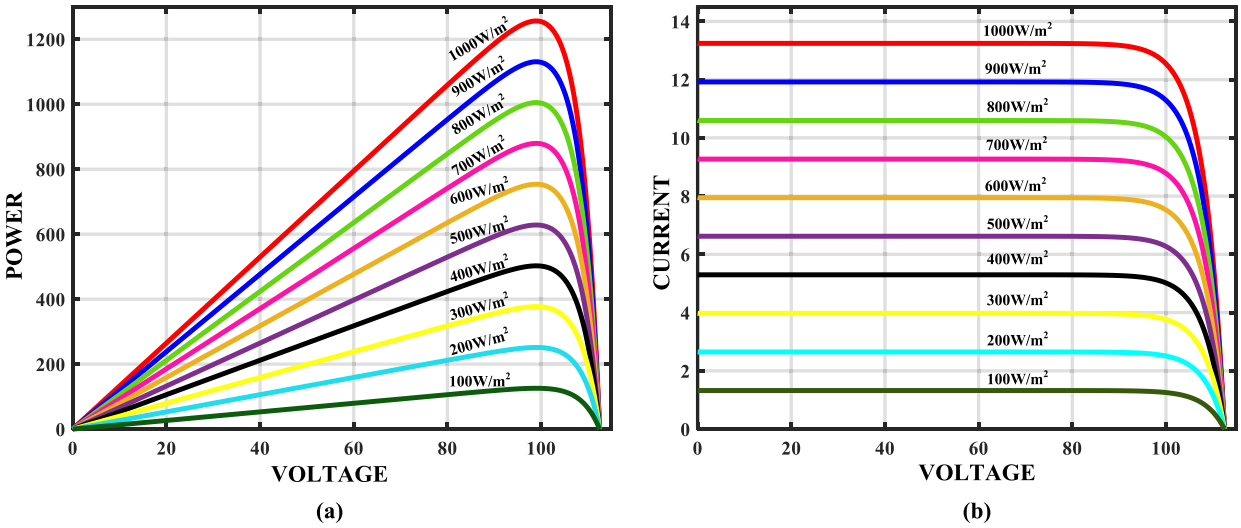

FIGURE 5. P-V and I-V characteristics vs solar irradiation.

TABLE 2. Specification of PV modules.

S. No	Parameters	Rating
1.	Maximum Power (P_m)	50Wp
2.	Maximum Power Voltage (V_m)	20V
3.	Maximum Power Current (I_m)	2.51A
4.	Short Circuit Current (I_{SC})	2.65A
5.	Open Circuit Voltage (V_{OC})	22.5V
6.	STC Irradiance (G_{STC})	1000W/m^2
7.	STC Temperature (T_{STC})	25ºC

and it can permanently damage the cell. As given the equation (3), the current generation and power output are directly proportional to the amount of irradiation received by the panel surface. At the standard test condition, (1000W/m^2), the panel generates the rated current, and when the irradiation is reduced to 100W/m^2 the panel generates 10% of the rated current. The power output concerning to the various amount of irradiation is simulated in the *MATLAB/Simulink*® model and the corresponding diagrammatic representation is shown in Figure 5. The P-V and I-V curves under the various irradiation levels were describes the characteristics of the PV system concerning the irradiation. The efficiency of the PV cell can be stated as, the ratio between the actual power output to the rated power generating capability of the PV cell, and the corresponding expression is given in equation (10)

$$Efficiency, \eta = \frac{P_m}{P_{STC}} \times 100\% \tag{10}$$

III. SIMULATION OF THE VARIOUS ARRAY CONFIGURATION SCHEMES

A 5 × 5 PV array is modeled in *MATLAB/Simulink*® to validate the various kinds of array configurations as shown in figure 6. The PV cell is developed and integrated as a 5×5 PV array based on the mathematical equation. Table 2 contains the PV module specifications.

The various array configurations like series configuration, parallel configuration, series-parallel array configuration, bridge linked array configuration, honeycomb array configuration, total cross tied array configuration, SuDoKu puzzle pattern array configuration, Futoshikii puzzle pattern array configuration, Magic Square array configuration, Competence square configuration, SD-PAR array configuration, Odd-Even Structure configuration, Chaotic Map Array configuration Dominance Square Configuration, Sky Crapper array configuration, L-Shape array configuration, and Screw pattern array configuration were analyzed in terms of power generation and efficiency. *MATLAB/Simulink*® is the tool used for modeling the above array configurations in the simulation and validation. For each PV array configuration, a 5 × 5 PV array is modeled using the single diode PV cell model's mathematical equation as shown in figure 7. The 5 × 5 PV array of each configuration is represented in the simulation model as blue blocks. The subsystem has three output terminals: maximum power output (Pm), open-circuit voltage (VOC), and short circuit current (ISC).

These terminals' discrete samples are presented to the workspace for comparison. Additionally, these data are plotted using the plotter block as the Power-Voltage (P-V) and Current-Voltage (I-V) characteristic curves. Various kinds of shading patterns are used to analyze the effectiveness of each array configuration. For all panels, the irradiation block has 25 irradiation values. Goto blocks are used to incorporate these irradiation values into each subsystem of the array configurations. The simulation results are obtained by applying the different shading pattern, PV solar panels do not receive constant illumination throughout the day. It changes throughout time, which is a normal occurrence. However, uneven irradiation/partial shading is occurred in PV systems due to the various elements like nearby objects, such as trees, towers, buildings, and clouds, among others. The pattern of these shades is not constant, and it is also unpredictable. Some

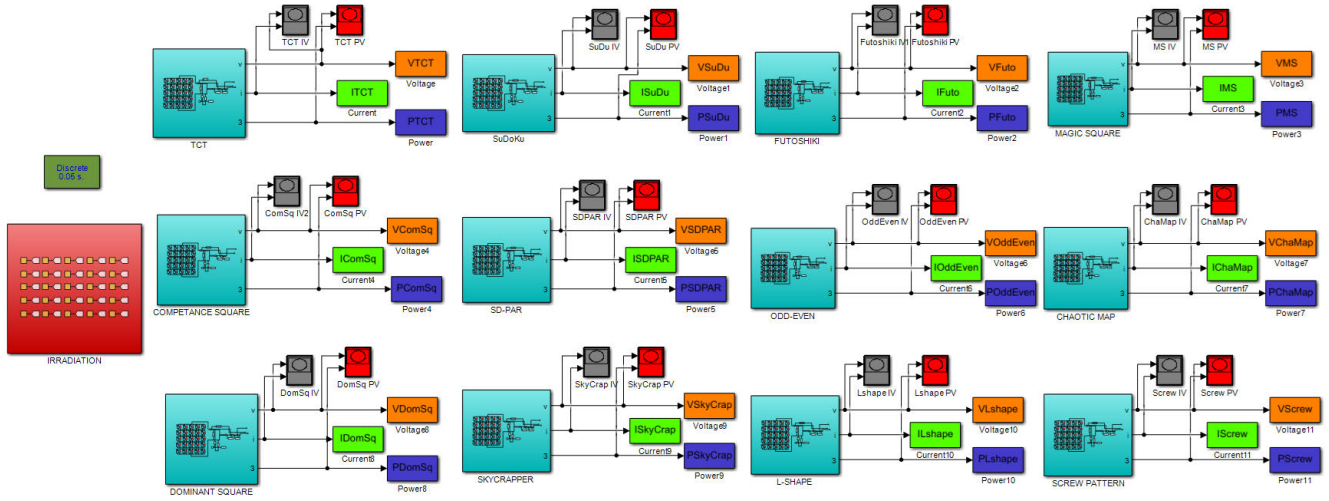

FIGURE 6. Simulation diagram of the various array configurations.

of the shading patterns, like newly constructed buildings, towers, etc., can be predicted and can be avoided by the proper arrangements. However, the shadings caused by clouds, dust buildup, bird droppings, etc., are unpredictable. These factors are causing the partial shadowing in the PV array. This operates the PV rows to function with the unequal current generation that leads to mismatch losses in the PV array. The mismatch loss is the difference between the maximum and least power-generating rows. The power production from PV modules that are in good condition and receive proper sunlight is limited by faulty or partially shaded PV modules. The faulty and partially shaded modules reduce the power output of the healthier modules. This leads to a mismatch loss. The most possible shading patterns occurring on the PV array can be divided into ten types of shading patterns based on the shading level. All kinds of shading levels (minimum to maximum) are coming under these ten kinds of shading patterns. These ten kinds of shading patterns are corner shading, center shading L-Shape shading Frame shading, diagonal shading, random shading, short and narrow (SN) shading, short and wide (SW) shading, Long and narrow (LW) shading, and long and wide (LW) shading. Under these ten shading patterns the performance of all PV array configurations is validated.

IV. TYPE OF SHADING PATTERNS

A. HEALTHY PATTERN

All PV modules in a 5 × 5 PV array are subjected to 1000W/m^2 under this shading pattern, which is shown in Figure 1.

B. CORNER SHADING PATTERN

The corner-positioned modules in a 5 × 5 PV array are subjected to various irradiance under this shading pattern, which is shown in Figure 8.

- PV15 module received an irradiation of 900W/m^2.
- PV11 and PV55 modules were received irradiation of 800W/m^2.
- PV51 module is received an irradiation of 400W/m^2.
- The remaining PV modules received 1000W/m^2.

C. CENTRE SHADING PATTERN

The center shading pattern shown in Figure 8 subjects the centrally located modules in a 5 × 5 PV array to varying levels of irradiance.

- PV43 module received an irradiation of 900W/m^2.
- PV32 and PV44 modules received irradiation of 800W/m^2.
- PV24 and PV42 modules received irradiation of 600W/m^2.
- PV23 and PV34 modules received irradiation of 400W/m^2.
- PV22 and PV33 modules received irradiation of 200W/m^2.
- The remaining PV modules received 1000W/m^2.

D. L-SHAPE SHADING PATTERN

The L-shape shading pattern shown in Figure 8 subjects the L-shaped located modules in a 5 × 5 PV array to varying levels of irradiance.

- PV31 module is received an irradiation of 900W/m^2.
- PV11 and PV55 modules received irradiation of 800W/m^2.
- PV41 and PV52 modules received irradiation of 600W/m^2.
- PV21 and PV53 modules received irradiation of 400W/m^2.
- PV51 and PV54 modules received irradiation of 200W/m^2.
- The remaining PV modules received 1000W/m^2.

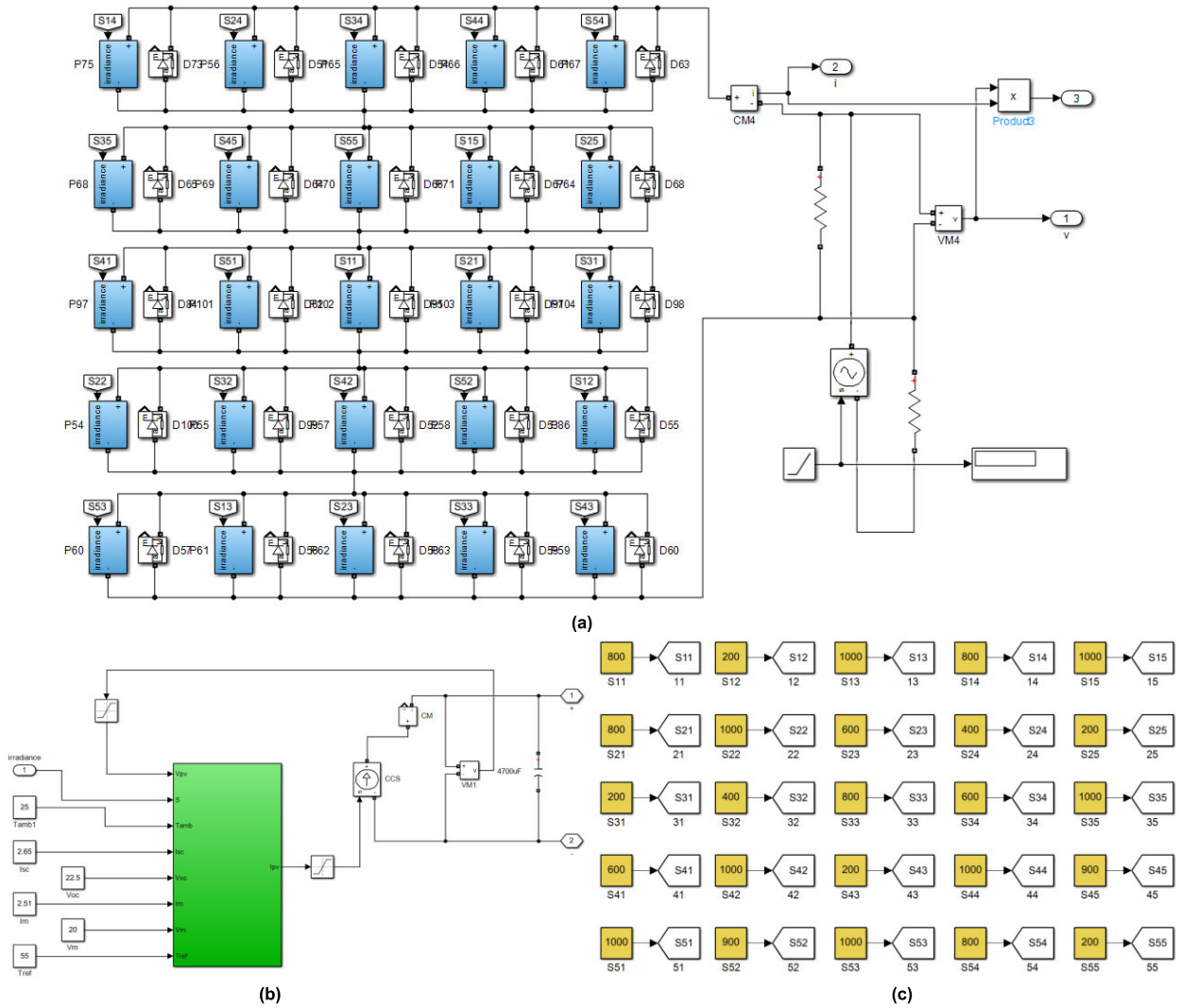

FIGURE 7. (a) Modeling of 5 × 5 PV array (b) Modeling of single PV module (c) Irradiation block in the simulation.

E. FRAME SHADING PATTERN

The frame shading pattern shown in Figure 8 subjects the PV modules on all edges to varying levels of irradiance.

- PV31 module received an irradiation of 900W/m^2.
- PV11 and PV55 modules received irradiation of 800W/m^2.
- PV41 and PV52 modules received irradiation of 600W/m^2.
- PV21 and PV53 modules received irradiation of 400W/m^2.
- PV51 and PV54 modules received irradiation of 200W/m^2.
- The remaining PV modules received 1000W/m^2.

F. DIAGONAL SHADING PATTERN

The diagonal shading pattern shown in Figure 8 subjects the diagonally located modules in a 5 × 5 PV array to varying levels of irradiance.

- PV55 module received irradiation of 900W/m^2.
- PV44 module received irradiation of 800W/m^2.
- PV22 module received irradiation of 600W/m^2.
- PV33 module received irradiation of 400W/m^2.
- PV11 module received irradiation of 200W/m^2.
- The remaining PV modules received 1000W/m^2.

G. RANDOM SHADING PATTERN

The random shading pattern shown in Figure 8 subjects the randomly located modules in a 5 × 5 PV array to varying levels of irradiance.

- PV11, PV45 and PV52 modules were received the irradiation of 900W/m^2.
- PV14, PV21, PV33 and PV54 modules were received the irradiation of 800W/m^2.
- PV23, PV34 and PV41 modules were received the irradiation of 600W/m^2.

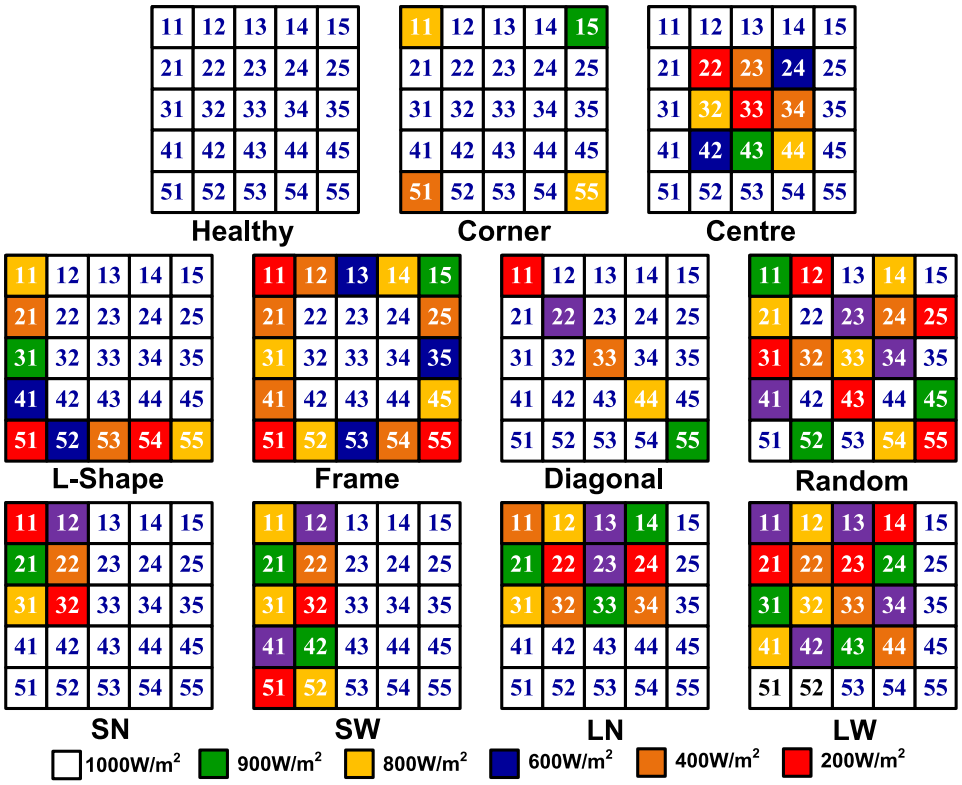

FIGURE 8. Various kinds of shading patterns used for the analysis.

- PV24 and PV32 modules received an irradiation of 400W/m^2.
- PV12, PV25, PV31, PV43, and PV55 modules were received the irradiation of 200W/m^2.
- The remaining PV modules received 1000W/m^2.

H. SHORT AND NARROW SHADING PATTERN

The shading pattern depicted in Figure 8 exposes the SN-positioned modules of a 5 × 5 PV array to varying levels of irradiance.

- PV21 module received an irradiation of 900W/m^2.
- PV31 module received irradiation of 800W/m^2.
- The PV12 module received irradiation of 600W/m^2.
- PV22 module received irradiation of 400W/m^2.
- PV11 and PV31 modules received irradiation of 200W/m^2.
- The remaining PV modules received 1000W/m^2.

I. SHORT AND WIDE SHADING PATTERN

The shading pattern depicted in Figure 8 exposes the SW-positioned modules of a 5 × 5 PV array to varying levels of irradiance.

- PV21 and PV42 modules received irradiation of 900W/m^2.
- PV11, PV31, and PV52 modules received the irradiation of 800W/m^2.
- PV12 and PV41 modules were received the irradiation of 600W/m^2.
- PV22 module received an irradiation of 400W/m^2.
- PV32 and PV51 modules received irradiation of 200W/m^2.
- The remaining PV modules received 1000W/m^2.

J. LONG AND NARROW SHADING PATTERN

The shading pattern depicted in Figure 8 exposes the LN-positioned modules of a 5 × 5 PV array to varying levels of irradiance.

- PV14, PV21, and PV33 modules received irradiation of 900W/m^2.
- PV12 and PV31 modules received irradiation of 800W/m^2.
- PV13 and PV23 modules received irradiation of 600W/m^2.
- PV11, PV32, and PV34 modules received irradiation of 400W/m^2.
- PV22 and PV24 modules received irradiation of 200W/m^2.
- The remaining PV modules received 1000W/m^2.

K. LONG AND WIDE SHADING PATTERN

The shading pattern depicted in Figure 8 exposes the LW-positioned modules of a 5 × 5 PV array to varying levels of irradiance.

- PV24, PV31, and PV43 modules received irradiation of 900W/m^2.
- PV12, PV32, and PV41 modules received irradiation of 800W/m^2.
- PV11, PV13, PV34, and PV42 modules received the irradiation of 600W/m^2.
- PV22, PV33, and PV44 modules received irradiation of 400W/m^2.
- PV14, PV21, and PV23 modules received irradiation of 200W/m^2.
- The remaining PV modules received 1000W/m^2

V. TYPES OF PV ARRAY CONFIGURATIONS

Many topologies for PV arrays have been developed to lessen power losses caused by partial shading. Depending on the array topology, partial shading in a PV system has different effects. Traditional PV array topologies like series, parallel, and series-parallel configurations are ineffective in partial shade. In this study, a brief comparison is given between the array configurations used from the initial stages to the present advanced techniques.

A. SERIES ARRAY CONFIGURATION ARRAY CONFIGURATION

Figure 9(a) depicts a series array setup. Because all the PV panels are connected in series, partial shade has a substantial impact on the PV array's output power [46], [47], [48], [49], [50]. Under Partial shading condition, the output current of the PV array is limited by the minimum current generating row, which leads to the mismatch loss. The shaded panels in the PV array have functioned with a reverse bias. As a result, the shaded panels begin to heat up and the power loss has taken place in the form of heat energy. This damages the PV panels. As a result, each PV panel has a bypass diode across it to prevent such hot areas. The accompanying bypass diode is forward biased when a particular panel experiences partial shading. Because of the bypass diode, the I-V and P-V characteristics of the PV array has many numbers of peaks.

B. PARALLEL ARRAY CONFIGURATION ARRAY CONFIGURATION

As seen in Figure 9(b), all the PV panels are connected in parallel in this parallel array configuration [46], [47], [48], [49], [50]. There are no multiple peaks in the P-V and I-V characteristics curves due to the parallel connections. Also, this array configuration performs better under partial shading conditions. But it experiences more power losses in the PV array due to the output current, where the output current in a parallel connection is the sum of each panel current. Furthermore, the parallel connection of all panels limits PV array voltage to a lower value. As a result, this topology is incompatible with many PV system applications.

C. 5.3 SERIES - PARALLEL (SE-P) ARRAY CONFIGURATION

As shown in Figure 9(c), some of the PV panels (with respect to number of rows) are connected in series to frame a PV string, and further these strings (with respect to number of columns) are connected in parallel to construct a Se-P array configuration [46], [47], [48], [49], [50]. A detailed simulation analysis for a 5 × 5 Series - Parallel array topology under various partial shading situations has been carried out and the corresponding observations were discussed in result and discussions section. This Se-P array configuration is the most extensively used configuration because of its dependability, viability, and minimal redundant connections. However, the amount of series connections makes partial shading more noticeable and increases mismatch loss. This topology's PV curve has more peaks when partially shaded. The Se-P array configuration generates more power than the conventional series and parallel topologies, but the MPPT controller used in the converter side failed to obtain the actual GMPP among the many numbers of LMPPs' in the occurrence of partial shading conditions.

D. BRIDGE LINKED (BL) ARRAY CONFIGURATION

A link has been include between the adjacent PV strings of Se-P array configuration can improve the power output and this type of linked configuration is called as the bridge linked array configuration. The array configuration of the BL configuration is shown in Figure 9 (d). The BL array configuration has been analyzed in the 5 × 5 PV array, and the corresponding observations were discussed in result and discussions section. Mismatch losses are larger in the BL topology than in the conventional TCT topology because it has fewer inter-link connections between neighboring strings. This BL array configuration has the better performance as compared to the series and Se-P array configurations [50].

E. HONEY COMB (HC) ARRAY CONFIGURATION

The modules of this topology are connected in the hexagon form of a honey comb arrangement, as seen in Figure 9 (e). This array configuration has the more numbers of interlinks between the PV strings, so that, the mismatch losses between the PV panels and the corresponding strings can be reduces. The HC array configuration has been modelled and analyzed in the 5 × 5 PV array, and the corresponding results were discussed in result and discussions section.

F. TOTAL CROSS TIED ARRAY CONFIGURATION(TCT)

Each PV panels are connected in series and parallel with the neighboring PV modules for constructing a Total Cross Tied (TCT) array configuration as shown in Figure 9(f). The TCT array configuration has the better performance as compared with the all the array configurations discussed above. This array configuration has many numbers of the interconnections which distributes the partial shading in the PV array. So accumulation of partial shading in a particular row or column can be avoided. The TCT array configuration has been constructed on a 5 × 5 PV array and analyzed under the various kinds of shading patterns. The corresponding results, P-V and I-V characteristic curves are shown in Figure 12. At the healthy shading pattern, the PV array constructed using

FIGURE 9. 5 × 5 PV array (a) Series (b) Parallel (c) Series-Parallel (d) Bridge-Linked (e) Honey Comb (f) Total Cross Tied array configurations.

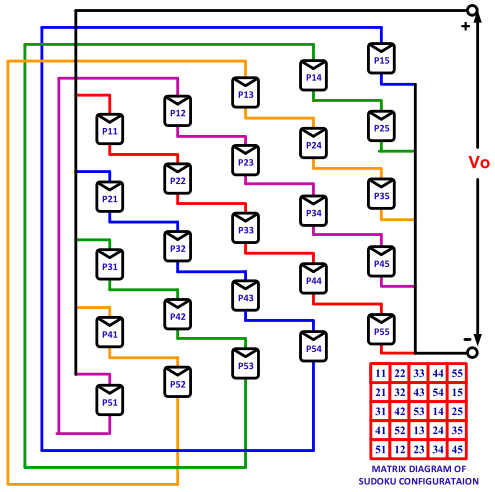

FIGURE 10. 5 × 5 SuDoKu array configuration establishment diagram.

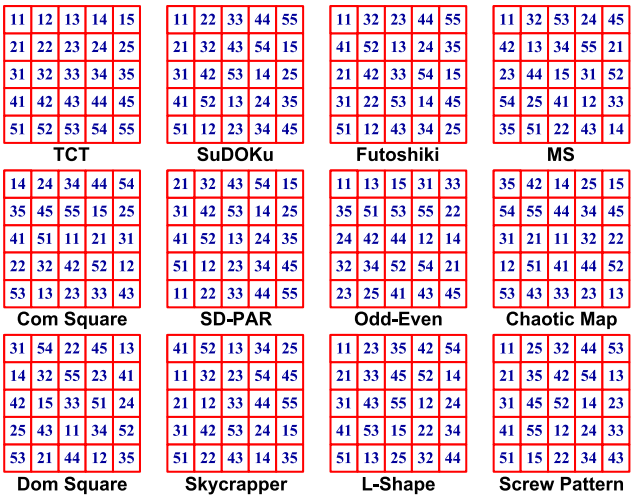

FIGURE 11. 5 × 5 PV array matrix diagram of the various array configurations.

the TCT array configuration generates rated power output. On the other complex shading pattern, the power output has decreased with respect to the shading pattern and shade dispersion rate.

G. SUDOKU PUZZLE PATTERN (SPP) BASED ARRAY CONFIGURATION

The SuDoKu is a logical number combination problem. The electrical connections between the PV panels are rearranged as per the number pattern created by the SuDoKu. These interconnections will not disturb the physical location of the PV modules. The change of interconnection has the high shade dispersion values as compared to the TCT configuration. Each PV row has been constructed using the different and unique PV modules from each row and column of the traditional array structure. This topology eliminates the two major problems of prior configurations: line losses and sub-array shading. The wiring between the PV modules should be minimum as much as possible for reducing the line losses.

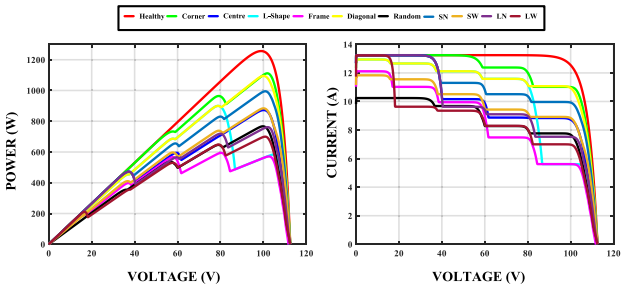

FIGURE 12. Characteristic curves of TCT under various shading patterns.

In SuDoKu configuration, it requires more length of wire for the execution of SuDoKu pattern [50], [51], [52], [53].

Under the various shading patterns, the characteristics curves of 5 × 5 array configuration is plotted as shown in Figure 13. At the healthy shading pattern, the PV array constructed using the SuDoKu puzzle pattern produces a STC power, however at the other shading pattern, the power output has decreased with respect to the shading patters and shade dispersion rate.

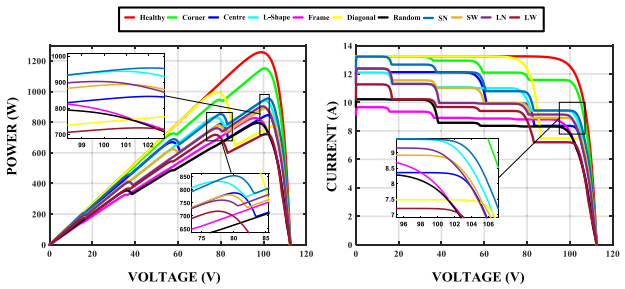

FIGURE 13. Characteristic curves of SuDoKu under various shading patterns.

H. FUTOSHIKI PUZZLE PATTERN (FPP) BASED ARRAY CONFIGURATION

In [54], a Futoshiki puzzle design arrangement is proposed. A logic-based puzzle with a n x n square grid is called futoshiki. In this puzzle, the digits 1 to n are arranged so that they appear once in each row and column of a square grid, without repeating. The puzzle has a singular solution since each digit must adhere to the inequality restriction between two adjacent integers that was first established before being placed in the square grid. The appropriate logic Futoshiki puzzle is generated using the linear programming technique (LPA), and it always has a unique solution in this reference paper. Figure 11 shows the matrix diagram of the 5 × 5 Futoshiki puzzle pattern-based PV array.

Under the various shading patterns, the performance of 5 × 5 array configuration is plotted as the P-V and I-V characteristics as shown in Figure 14, At the healthy shading pattern, this array configuration produces the rated STC power output. At the other shading pattern, the power output has decreased with respect to the shading patterns and shade dispersion rate.

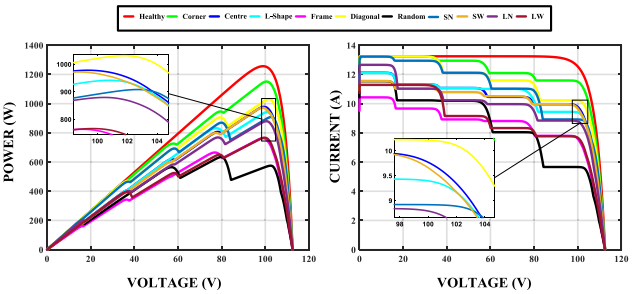

FIGURE 14. Characteristic curves of futoshiki under various shading patterns.

I. MAGIC SQUARE (MCSQ) BASED ARRAY CONFIGURATION

For extracting maximum power from the PV array, [55] applies Magic Square (MS), (a logic-based number placement problem) pattern. A magic square is the obtainment of the numbers 1 to n in a ''n×n'' matrix, where each number only appears once and also, the sum of the number in any row, column, or diagonal must be the same. The matrix dispersion diagram of the magic square-based array configuration is shown in Figure 11. This magic square arrangement may also be used with other large-sized PV arrays, such the 10 × 10, 14 × 14, and 18 × 18 arrays. This kind of array configuration reduces the mismatch losses as compared to other conventional array configurations. When compared to the traditional TCT arrangement, the magic square pattern performs better, avoids the need for complicated MPPT algorithms, and produces smoother PV array characteristics with fewer LMPP, which lessens the mismatch impact.

Under the various shading patterns, the behavior of 5 × 5 array configuration is plotted as the P-V and I-V characteristics as shown in Figure 15. This MS array configuration generates the rated power output at the STC values. When the system experiences the shading patterns, the power output has been reduced. However, this MS array configuration has the better performance as compared to other configurations.

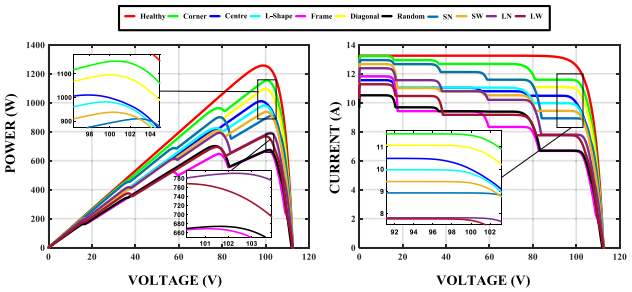

FIGURE 15. Characteristic curves of magic square under various shading patterns.

J. COMPETENCE SQUARE (CPSQ) BASED ARRAY CONFIGURATION

In [56] a new kind of array configuration based on the Competence Square (CpSq) method is introduced. This method

rearranges the PV modules by physically moving PV panels around in a TCT interconnection. This approach is a one-time relocation procedure that moves the PV panels according to a certain numerical pattern. The configuration is very simple to compute and it can be used to PV arrays of any size. The results shows that the CpSq approach outperforms the TCT and Dominance Square (DmSq) procedures in terms of performance. Figure 11 shows the matrix dispersion diagram of a 5 × 5 Competence square based PV array.

The competence square based array configuration has been constructed in the 5 × 5 PV array. This PV array has been validated under the different shading patterns and the corresponding P-V and I-V characteristic curves were presented in Figure 16. The array configuration has performed better than the TCT, Se-P but failed to perform better than the MS and SuDoKu based array configurations.

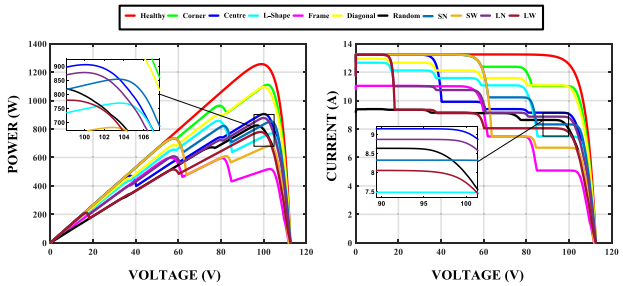

FIGURE 16. Characteristic curves of competence square under various shading patterns.

K. SHADE DISPERSION PHYSICAL ARRAY RELOCATION (SD-PAR) BASED ARRAY CONFIGURATION

The static shade dispersion physical array relocation (SD-PAR) method has been introduced for constructing the PV array in order to enhance the power output [57], [58]. This array configuration minimizes the mismatch losses and power losses by dispersing the influence of partial shading over the PV array. This method minimizes the power loss during partial shading by reducing the number of shaded modules in a row. The interconnections between the PV modules are changed without changing the physical location of the PV modules. A simulation is carried out to analyze the SD-PAR technique's performance for 5 × 5 PV array under various partial shading patterns. Additionally, the performance of this array configuration is compared with the other conventional array configurations, including Series-Parallel (SP), Bridge-Linked (BL), and Total Cross Tied (TCT).

The P-V and I-V characteristic curves of this array configuration under the various shading patterns were plotted as shown in Figure 17. Under the partial shading condition, the performance of this configuration has been reduced with respect to the shade dispersion level. This array configuration has the better shade dispersion capability.

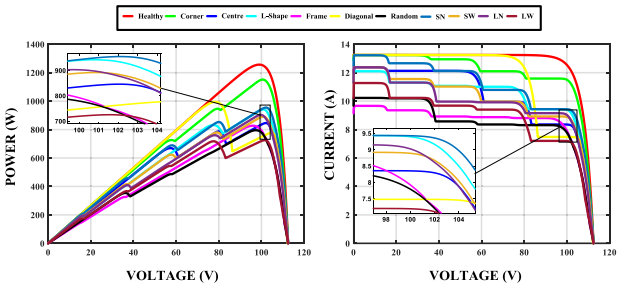

FIGURE 17. Characteristic curves of SD-PAR under various shading patterns.

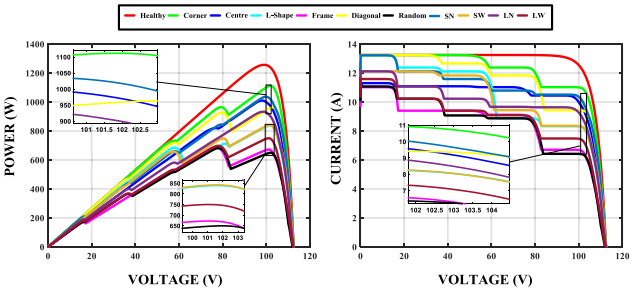

FIGURE 18. Characteristic curves of odd-even under various shading patterns.

L. ODD–EVEN (OE) PROPAGATION BASED ARRAY CONFIGURATION

In [59], an Odd-Even PV array configuration is presented for enhancing the performance of the PV systems. This configuration selects the odd-odd, odd-even, even-even, and even-odd propagation for obtaining the position of the PV modules in each row and column. This configuration rearranges the interconnections of the PV array based on the pattern framed by the odd-even propagation. This type of configuration selects the PV modules with the even and optimal distance which reduces the required quantity of wires. So that the line losses associated in the PV array can be reduced. The PV array can be built with any number of rows and columns (symmetrical or asymmetrical) by using this method. This method eliminates the complicated logics behind the PV array formations as logics used in other configurations. This type of array configuration is constructed in a 5 × 5 PV array and it was validated under the various shading conditions. The author's stats that this array structure is simpler, more effective, and affordable. However, the performance of this PV array can be enhanced more by the other configurations like L-shape, screw pattern, MS. Figure 11 shows the matric dispersion diagram of the Odd-Even structure-based array configuration. The P-V and I-V characteristic of this array configuration under the various kinds of shading pattern is shown in Figure 18.

M. CHAOTIC MAP (CHMP) BASED ARRAY CONFIGURAITON

In order to lessen mismatch power losses driven on by partial shade, [60] proposed the Chaotic Baker Map (CBM) approach. By spreading the partial shade effect throughout the full array without altering its electrical connections, this method decreases power loss. The array methodology is implemented in for 5 × 5 PV Array, and the performance has been evaluated and compared with the of conventional and recently developed array configurations such as Series Parallel, Total Cross Tied, Bridge Link, and Honey Comb arrangements.

This approach does not follow any kinds of complicated algorithms and it has an enhanced power output with the lower mismatch losses. This design is appropriate for large-scale solar installations and Building Integrated PV (BIPV) systems. Under the various shading patterns, the behavior of 5 × 5 array configuration is plotted as the P-V and I-V characteristics as shown in Figure 19.

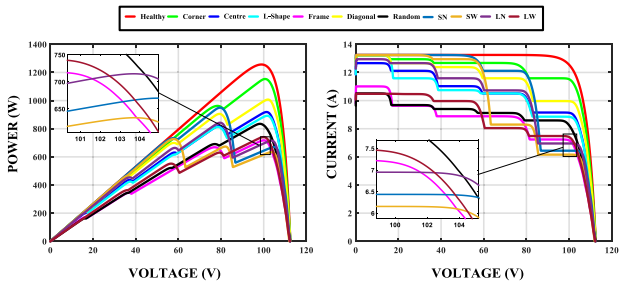

FIGURE 19. Characteristic curves of chaotic map under various shading patterns.

N. DOMINANCE SQUARE (DMSQ) BASED ARRAY CONFIGURAITON

Dominance Square based array configuration [61] is presented for enhancing the performance of the solar PV array. The ordinary Total Cross Tied (TCT) configurations has been configured using this dominance square approach. The PV modules positions in each row and column has been rearranged for obtaining this array configuration. The logic used in this approach is mostly similar to the competence square based array configuration. This approach has almost similar performance to the CS based array configuration.

As compared with the conventional methods, this approach has the better efficiency. The matrix dispersion diagram of this array configuration is shown in Figure 11. The P-V and I-V characteristic curves of this approach has been obtained under the various shading patterns as shown in Figure 20.

O. SKYSCRAPER(SYC) BASED ARRAY CONFIGURATION

Skyscraper puzzle-based one-time reconfiguration solution [62] is developed for all kinds of PV array. This array configuration efficiently tackles problems like high computational burden, flexibility to expand high or low array size, and time-consuming connector links and etc., The height of

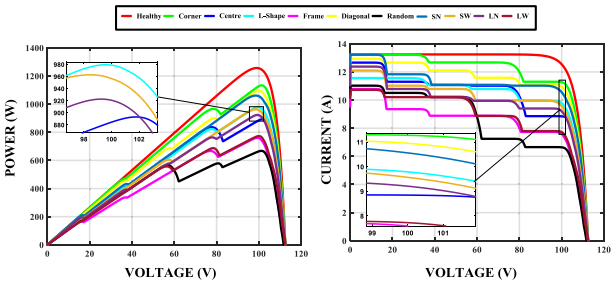

FIGURE 20. Characteristic curves of dominance square under various shading patterns.

several buildings that can be viewed from a single point of view. Like that, in the row formation of the PV array can be viewed on each dimensional for obtaining the PV module positions. This array configuration method has been modelled in a 5 × 5 PV array and the performance has been validated in the different kinds of shading patterns. The matrix dispersion diagram of this array configuration has shown in Figure 11. The validation under the different shading patterns has been plotted as the P-V and I-V characteristic curves and it shown in Figure 21. This method outperforms the other PV array configurations like Total Cross Tie connection, the Dominance Square, and SuDoKu methods, in terms of shade distribution and power generation.

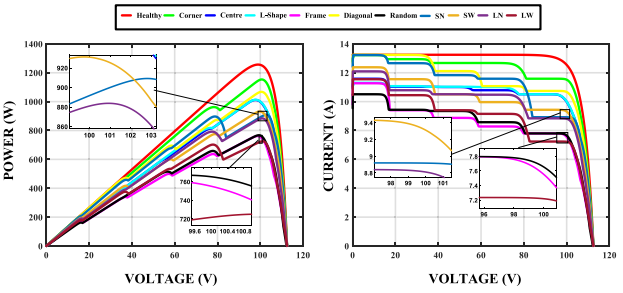

FIGURE 21. Characteristic curves of sky scrapper under various shading patterns.

P. L-SHAPE PROPAGATED ARRAY CONFIGURAITON

The logic puzzles like SuDoku and futoshiki are suitable only for the squared PV array. But these logics were failed and doesn't work for the non-square PV array. The L-shaped array configurations [63] presented a new kind of array configuration based on the moment of the knight coin of the chess game. For the non-squared PV array, this L-shape propagated array configuration constructs the PV array with the repeated PV modules with the optimal distance from the same row or same column. So that, this L-shape propagated array configuration can be implemented for both square and non-squared PV array.

This kind of PV array configuration has created the PV rows by the L propagation from the starting node and continuing until it reaches the final column or the column before it. The L propagation should stop when it reaches the last or

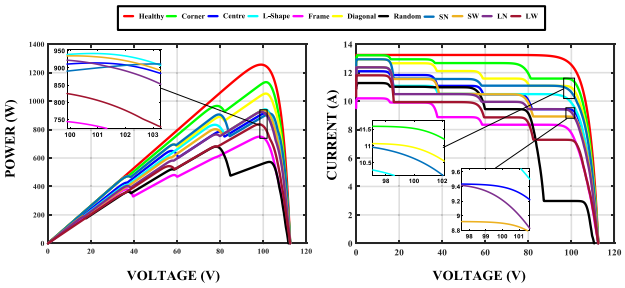

FIGURE 22. Characteristic curves of l-shape under various shading patterns.

prior column of the PV array and then restart from the second column of the PV row until it reaches the end. As a result, the PV rows has been constructed with individual PV panels from each row or repeating PV panels spaced at the optimum distance. The propagation factors is the key for considering the starting node and its related column. In comparison to SuDoKu, this array construction significantly lowers the mismatch losses in the PV system. The matrix dispersion diagram of the 5×5 L-shape propagated array configuration is shown in Figure 11. The performance of this array configuration has been validated under the various shading patterns and the corresponding P-V and I-V characteristic curves were obtained as shown in Figure 22. As compared to conventional array configurations like Se-P, TCT, SuDoKu, MS, DC, CS, this L-shape array configuration generates maximum power with lesser mismatch losses. As compared to other configurations, this configuration disperses the shading uniformly over the PV array.

Q. SCREW PATTERN PROPAGATED ARRAY CONFIGURATION

Based on the screw structure, the screw pattern array configuration is implemented in [64]. This propagation enables the PV array to provide the PV modules with the optimal spacing between each one. For instance, each row of the typical PV array is built using unique PV modules from the various rows. The screw pattern-based array configuration can be divided into two types like horizontal and vertical screw pattern array configuration. The type of propagation can also divide into odd propagation and even propagation. When deciding on the type of array propagation, the size of the PV array must be considered.

VI. RESULTS AND DISCUSSIONS

There are ten kinds of different shading patterns are considered for the validation of these array configurations. These shading patterns can be classified into two categories such as mild shading pattern and severe shading pattern. The severe shading is causing more power losses in the PV system as compared to the mild shading patterns. The diagonal shading pattern, random shading pattern, short and narrow shading, short and wide shading pattern, long and narrow shading pattern, long and wide shading pattern are coming under the severe shading type and the other shading patterns are coming under the mild shading patterns. The performance of the various array configurations [Series, Parallel, Series-Parallel, TCT, SuDoKu, Futoshiki, Magic square, Competence Square, SD-Par, Odd-Even, Chaotic map, Dominant square, Sky Crapper, L-Shape propagated and screw propagated configuration were analyzed under the severe shading patterns. All the PV array configurations are generating the rated power output on the healthy operating condition. Under the corner shading pattern, the SPP, FPP.McSq, SyC, LSP array configurations are generating similar power output of 1054W, with the 84.3% of efficiency. This configuration performs better than the other PV configurations. The SCP and DmSq array configurations generate the second highest power generation of 1029W. The series array configuration has the least power generation of 251W power in the all cases of shading patterns. In the series connection all PV modules are connected in series connection where, the least power generating PV module will limits the power generation of other PV modules. This is the major drawback in the series array configurations.

On other hand, the parallel array configuration produces a more power than the all-recent array topologies. But the parallel array configuration is not feasible for the large PV system. When the PV cells are connected in parallel, the current output will be increased which increases the complexity in the power processing units. For handling the highest current, the proper safety precautions are mandatory. Also, high rated elements are required for the power conversion units. Due these constraints, the parallel array configuration is not preferable for the large power systems. Under the centre shading condition, the McSq and SyC array configurations were produces the maximum power output of 1004W with 80.3% of efficiency, where these array configurations are effectively distributing the shading in the PV array. The LSP array configuration has the second highest power generation of 904W power with 72.3% of efficiency. The series parallel array configuration has generated the least power generation of 703W power with the efficiency of 56.2%. The SyC array configuration produces the maximum power of 1004W with the efficiency of 80.3% in the L-Shape shading patterns. Series parallel and TCT array configuration has the least power generation of 552W power. In this shading condition, the performance of CpSq and ChMp array configurations were decreased due to the poor shade dispersion rate

The SPP and SD-PAR array configurations are failed to disperse the shading equally in the PV system, which leads to the least power generation. The FPP, OE and ChMp array configuration were quite capable to perform averagely in this kind of shading pattern. Under the random shading pattern, the LSP array configuration failed to disperse the shading as it causes the minimum power generation of 301W. The other configuration like, S, P, Se-P, TCT, SPP, FPP. McSq, CpSq, SD-PAR. OE, ChMp, DmSq, SyC and SCP array configuration were generating the power output of 251W, 869W, 301W, 703W, 778W, 703W, 653W, 828W, 778W,

TABLE 3. Performance of various array configurations under healthy shading pattern.

S.No	Array Configuration	Row Current, I_{ROW} (A)					Short Circuit Current, I_{SC} (A)	Maximum Power Output, P_M (W)	Efficiency, η (%)
		I_{R1}	I_{R1}	I_{R1}	I_{R1}	I_{R1}			
1.	Series	2.65	-	-	-	-	2.65	1250	100
2.	Parallel	66.25	-	-	-	-	66.25	1250	100
3.	Series-Parallel	2.65	2.65	2.65	2.65	2.65	13.25	1250	100
4.	TCT	13.25	13.25	13.25	13.25	13.25	13.25	1250	100
5.	SuDoKu	13.25	13.25	13.25	13.25	13.25	13.25	1250	100
6.	Futoshiki	13.25	13.25	13.25	13.25	13.25	13.25	1250	100
7.	Magic Square	13.25	13.25	13.25	13.25	13.25	13.25	1250	100
8.	Com. Square	13.25	13.25	13.25	13.25	13.25	13.25	1250	100
9.	SD-PAR	13.25	13.25	13.25	13.25	13.25	13.25	1250	100
10.	Odd-Even	13.25	13.25	13.25	13.25	13.25	13.25	1250	100
11.	Chaotic Map	13.25	13.25	13.25	13.25	13.25	13.25	1250	100
12.	Dom. Square	13.25	13.25	13.25	13.25	13.25	13.25	1250	100
13.	Sky Crapper	13.25	13.25	13.25	13.25	13.25	13.25	1250	100
14.	L-Shape	13.25	13.25	13.25	13.25	13.25	13.25	1250	100
15.	Screw Pattern	13.25	13.25	13.25	13.25	13.25	13.25	1250	100

TABLE 4. Performance of various array configurations under corner shading pattern.

S.No	Array Configuration	Row Current, I_{ROW} (A)					Short Circuit Current, I_{SC} (A)	Maximum Power Output, P_M (W)	Efficiency, η (%)
		I_{R1}	I_{R1}	I_{R1}	I_{R1}	I_{R1}			
1.	Series	0.53	-	-	-	-	0.53	251	20.1
2.	Parallel	61.75	-	-	-	-	61.75	1170	93.6
3.	Series-Parallel	0.53	2.65	2.65	2.65	2.12	10..6	1004	80.3
4.	TCT	11.4	13.25	13.25	13.25	10.6	10.6	1004	80.3
5.	SuDoKu	11.13	12.9	13.25	13.25	11.13	11.13	1054	84.3
6.	Futoshiki	11.13	13.25	12.9	13.25	11.13	11.13	1054	84.3
7.	Magic Square	11.66	12.72	12.9	13.25	11.13	11.13	1054	84.3
8.	Com. Square	13.25	12.45	9.54	13.25	13.25	9.54	904	72.3
9.	SD-PAR	12.9	13.25	13.25	11.13	11.13	11.13	1054	84.3
10.	Odd-Even	11.4	10.6	13.25	13.25	13.25	10.6	1004	80.3
11.	Chaotic Map	12.9	12.72	11.66	11.13	13.25	9.54	904	72.3
12.	Dom. Square	13.25	12.72	10.9	11.66	13.25	10.9	1029	82.3
13.	Sky Crapper	13.25	11.66	12.72	12.9	11.13	11.13	1054	84.3
14.	L-Shape	11.66	13.25	12.72	12.9	11.13	11.13	1054	84.3
15.	Screw Pattern	11.66	13.25	13.25	12.72	10.9	10.9	1029	82.3

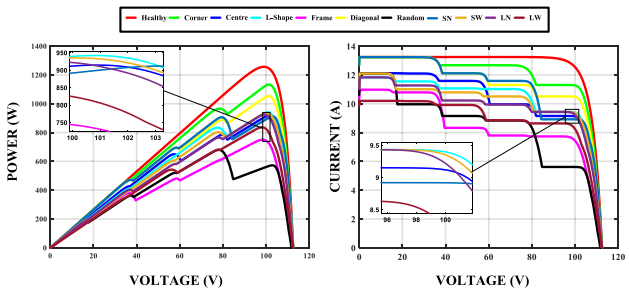

FIGURE 23. Characteristic curves of SCP configuration under various shading patterns.

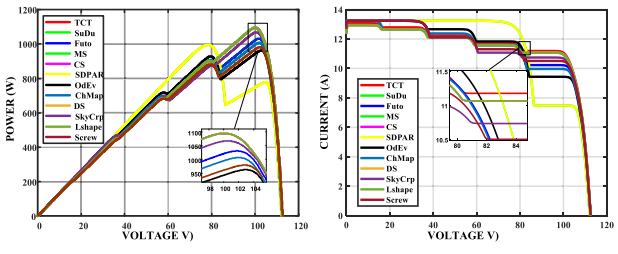

FIGURE 24. Characteristic curves of PV array configurations under random shading pattern.

628W, 828W, 653W, 753W and 552W respectively. Among these configurations the CpSq and ChMp array configuration produces the maximum power output and other configuration produces the average power output under this random shading pattern. Under the short and narrow shading pattern, the

TABLE 5. Performance of various array configurations under centre shading pattern.

S.NO	Array Configuration	Row Current, I_{ROW} (A)					Short Circuit Current, I_{SC} (A)	Maximum Power Output, P_M (W)	Efficiency, η (%)
		I_{R1}	I_{R1}	I_{R1}	I_{R1}	I_{R1}			
1.	Series	0.53	-	-	-	-	0.53	251	20.1
2.	Parallel	55.4	-	-	-	-	55.4	1049	83.9
3.	Series-Parallel	2.65	0.53	0.53	1.06	2.65	7.42	703	56.2
4.	TCT	13.25	8.48	9.01	11.4	13.25	8.48	803	64.3
5.	SuDoKu	8.48	12.5	12.2	12.2	10.1	8.48	803	64.3
6.	Futoshiki	10.6	12.2	10.1	11.13	11.7	10.1	954	76.3
7.	Magic Square	12.2	10.6	11.13	11.13	10.9	10.6	1004	80.3
8.	Com. Square	10.1	13.25	13.25	9.5	9.3	9.3	879	70.3
9.	SD-PAR	12.5	12.2	12.2	10.1	8.48	8.48	803	64.3
10.	Odd-Even	11.13	11.13	10.6	11.13	11.4	10.6	1004	80.3
11.	Chaotic Map	12.2	11.13	10.6	12.7	9.3	9.3	879	70.3
12.	Dom. Square	11.13	11.13	9.01	11.4	12.7	9.01	853	68.3
13.	Sky Crapper	11.7	11.13	10.6	11.13	10.9	10.6	1004	80.3
14.	L-Shape	10.6	11.13	11.9	9.54	12.2	9.54	904	72.3
15.	Screw Pattern	12.2	12.2	11.7	10.1	9.3	9.3	879	70.3

TABLE 6. Performance of various array configurations under l-shape shading pattern.

S.No	Array Configuration	Row Current, I_{ROW} (A)					Short Circuit Current, I_{SC} (A)	Maximum Power Output, P_M (W)	Efficiency, η (%)
		I_{R1}	I_{R1}	I_{R1}	I_{R1}	I_{R1}			
1.	Series	0.53	-	-	-	-	0.53	251	20.1
2.	Parallel	54.9	-	-	-	-	54.9	1039	83.1
3.	Series-Parallel	0.53	1.59	1.06	0.53	2.12	5.83	552	44.2
4.	TCT	12.7	11.13	12.9	12.2	5.83	5.83	552	44.2
5.	SuDoKu	12.2	9.01	11.4	11.13	11.13	9.01	853	68.3
6.	Futoshiki	12.19	11.13	9.01	11.4	9.5	9.01	853	68.3
7.	Magic Square	11.13	10.6	11.9	10.1	11.13	10.1	954	76.3
8.	Com. Square	11.13	12.7	7.2	12.3	11.7	7.2	678	54.2
9.	SD-PAR	9.01	11.4	11.13	11.13	12.2	9.01	853	68.3
10.	Odd-Even	12.5	9.01	13.3	7.95	12.2	7.95	753	60.2
11.	Chaotic Map	13.25	10.6	10.3	6.9	11.7	6.9	653	52.2
12.	Dom. Square	10.9	11.7	11.13	11.7	9.5	9.5	904	72.3
13.	Sky Crapper	11.13	10.6	10.6	11.4	11.13	10.6	1004	80.3
14.	L-Shape	10.6	10.1	12.5	10.6	11.13	10.1	954	76.3
15.	Screw Pattern	11.13	9.01	11.9	11.7	11.13	9.01	853	68.3

LSP, DmSq and McSq array configuration were performs well and has the higher power generation as compared to the other PV configurations. The ChMp array configuration falls short under this shading pattern, where all the shadings are accumulated in a single row that increases the mismatch losses between the rows. This affects the power generation of the PV array, where it produces the least power generation as compared to the other PV array configurations. Other configurations like SyC, CmSq, McSq, and Se-P array configurations were moderately performing under this shading pattern. The TCT array configuration produces a the 1004W of power output under the short and wide shading pattern, which is higher than the other configuration under this shading pattern. All array configurations except series array configuration are decently dispersing the shading in this shading pattern. Under the long and narrow shading pattern, McSq array configuration produces a maximum power output of 979W. The SCP, LSP, DmSq, OE, configurations were generating the second highest power output of 903W. On comparing the performance, the Se-P and ChMp array configurations had the poor performance in this kind of shading pattern. The SCP array configuration produces the highest power output of 66.3W with the efficiency of 66.3%, whereas the TCT array configuration minimum power generation of 678W power. The FPP, McSq, CpSq, and DmSq array configurations were produces the equal and moderate power generation of 753W. The performance of each array configuration can be easily studied using the P-V and I-V characteristic curves as given in figures. The smoothness of curves shows the uniform shade distribution. These characteristic curves are

TABLE 7. Performance of various array configurations under frame shading pattern.

S.No	Array Configuration	Row Current, I_{ROW} (A)					Short Circuit Current, I_{SC} (A)	Maximum Power Output, P_M (W)	Efficiency, η (%)
		I_{R1}	I_{R1}	I_{R1}	I_{R1}	I_{R1}			
1.	Series	0.53	-	-	-	-	0.53	251	20.1
2.	Parallel	46.4	-	-	-	-	46.4	879	70.3
3.	Series-Parallel	0.53	1.06	1.59	1.06	0.53	4.8	452	36.1
4.	TCT	7.7	10.1	11.66	11.13	5.83	5.83	552	44.2
5.	SuDoKu	9.01	9.81	9.54	9.01	9.01	9.01	853	68.3
6.	Futoshiki	9.01	9.01	9.81	10.6	6.89	6.89	653	52.2
7.	Magic Square	7.95	8.48	11.93	6.89	9.54	6.89	563	52.2
8.	Com. Square	11.13	7.69	5.3	11.13	11.13	5.3	502	40.2
9.	SD-PAR	9.81	9.54	9.01	9.01	9.01	9.01	853	68.3
10.	Odd-Even	9.28	6.89	11.13	9.54	9.54	6.89	653	52.2
11.	Chaotic Map	9.81	9.01	9.01	7.42	11.13	7.42	703	56.2
12.	Dom. Square	9.54	9.01	10.87	9.01	7.95	7.95	753	60.2
13.	Sky Crapper	8.48	9.01	7.95	11.39	9.54	7.95	753	60.2
14.	L-Shape	8.48	10.1	9.01	10.34	8.48	8.48	803	64.3
15.	Screw Pattern	8.48	7.95	11.13	7.95	10.87	7.95	753	60.2

TABLE 8. Performance of various array configurations under diagonal shading pattern.

S.No	Array Configuration	Row Current, I_{ROW} (A)					Short Circuit Current, I_{SC} (A)	Maximum Power Output, P_M (W)	Efficiency, η (%)
		I_{R1}	I_{R1}	I_{R1}	I_{R1}	I_{R1}			
1.	Series	0.53	-	-	-	-	0.53	251	20.1
2.	Parallel	60.7	-	-	-	-	60.7	1150	92
3.	Series-Parallel	0.53	1.59	1.06	2.12	2.39	7.69	728	58.2
4.	TCT	11.13	12.19	11.66	12.72	12.98	11.13	1054	84.3
5.	SuDoKu	7.69	13.25	13.25	13.25	13.25	7.69	728	58.2
6.	Futoshiki	10.34	13.25	11.66	12.19	13.25	10.34	979	78.3
7.	Magic Square	11.13	12.98	12.72	11.66	12.19	11.13	1054.	84.3
8.	Com. Square	12.72	12.98	11.13	12.19	11.66	11.13	1054	84.3
9.	SD-PAR	13.25	13.25	13.25	13.25	7.68	7.68	728	58.2
10.	Odd-Even	9.54	11.93	12.72	13.25	13.25	9.54	903	76.3
11.	Chaotic Map	13.25	12.46	10.1	12.72	11.66	10.1	954	72.3
12.	Dom. Square	12.19	12.98	11.66	11.13	12.72	11.13	1054	84.3
13.	Sky Crapper	13.25	11.13	10.87	13.25	12.19	10.87	1029	82.3
14.	L-Shape	11.13	11.66	12.98	12.19	12.72	11.13	1054	84.3
15.	Screw Pattern	10.6	13.25	13.25	11.4	12.19	10.6	1004	80.3

varied with respect to the array configurations. In many cases the recent developed array configurations have the smoother PV curve than the others. Under the mild shading patterns, the basic array configuration to recent array configurations were generating nearby power output. But on the case of severe shading patterns, some of the array configurations were failed to disperse the shading. By comparing the overall performance of each PV array configurations with respect to the all-shading patterns, the magic square array one of the best among other. Dominant Square, Sky Crapper array configuration are the second efficient configurations among the others in terms of shade dispersion and power generation. The L-Shape propagated array configuration and screw propagated array configuration are the performing good next to the DmSq and SyC array configurations. Series-Parallel array configuration has the least performance among the other PV array configurations on the shade dispersion rate. This configuration is highly limited by the shaded panel that leads to the high mismatch loss. This causes the power loss in the PV system. The TCT array configuration performs well in mild and medium shading patterns, but experiences more mismatch losses in complex shading patterns. The TCT configuration is the base for recently created array configurations such as SuDoKu, Futoshiki, CS, MS, DS, SD-PAR, L-shape, and screw. Because these configurations used separate logics but shared a same architecture of TCT. This is one of the reasons for the PV array's efficient shade dispersion in the recently developed array configurations. The traditional TCT experiences more mismatch losses in complex shading patterns, however the logics employed in recent configurations

TABLE 9. Performance of various array configurations under random shading pattern.

S.No	Array Configuration	Row Current, I_{ROW} (A)					Short Circuit Current, I_{SC} (A)	Maximum Power Output, P_M (W)	Efficiency, η (%)
		I_{R1}	I_{R1}	I_{R1}	I_{R1}	I_{R1}			
1.	Series	0.53	-	-	-	-	0.53	251	20.1
2.	Parallel	45.8	-	-	-	-	45.8	869	69.5
3.	Series-Parallel	0.53	0.53	0.53	1.06	0.53	3.18	301	24.1
4.	TCT	10.34	7.95	7.42	9.81	10.34	7.42	703	56.2
5.	SuDoKu	10.34	8.48	8.48	10.34	8.22	8.22	778	62.2
6.	Futoshiki	8.22	10.34	11.66	10.34	7.42	7.42	703	56.2
7.	Magic Square	1034	9.01	9.81	6.89	10.6	6.89	653	52.2
8.	Com. Square	9.01	8.75	9.23	9.23	9.54	8.75	828	66.3
9.	SD-PAR	8.48	8.48	10.34	8.22	10.34	8.22	778	62.2
10.	Odd-Even	10.34	11.13	9.01	8.75	6.63	6.63	628	50.2
11.	Chaotic Map	10.6	8.75	8.75	11.39	9.54	8.75	828	66.3
12.	Dom. Square	10.34	6.89	11.13	6.89	10.6	6.89	653	52.2
13.	Sky Crapper	8.22	9.54	7.95	9.54	10.6	7.95	753	60.2
14.	L-Shape	11.39	11.13	3.18	10.6	9.54	3.18	301	24.1
15.	Screw Pattern	9.28	12.2	9.01	5.83	9.54	5.83	552	44.2

TABLE 10. Performance of various array configurations under SN shading pattern.

S.No	Array Configuration	Row Current, I_{ROW} (A)					Short Circuit Current, I_{SC} (A)	Maximum Power Output, P_M (W)	Efficiency, η (%)
		I_{R1}	I_{R1}	I_{R1}	I_{R1}	I_{R1}			
1.	Series	0.53	-	-	-	-	0.53	251	20.1
2.	Parallel	58.57	-	-	-	-	58.57	1110	88.8
3.	Series-Parallel	0.53	0.53	2.65	2.65	2.65	9.01	853	68.3
4.	TCT	10.07	11.39	10.6	13.25	13.25	10.07	954	76.3
5.	SuDoKu	9.54	10.87	12.72	13.25	12.19	9.54	904	72.3
6.	Futoshiki	9.01	13.25	12.99	11.13	12.19	9.01	853	68.3
7.	Magic Square	11.13	12.99	12.72	12.19	11.66	11.13	1054	84.3
8.	Com. Square	13.25	13.25	10.34	8.48	13.25	8.48	803	64.3
9.	SD-PAR	10.87	12.72	13.25	12.19	9.54	9.54	903.6	72.3
10.	Odd-Even	10.6	11.67	12.19	10.87	13.25	10.6	1004	80.3
11.	Chaotic Map	13.25	13.25	6.63	12.99	13.25	6.63	628	50.2
12.	Dom. Square	11.13	11.13	13.25	11.13	11.93	11.13	1054	84.3
13.	Sky Crapper	13.25	9.01	11.93	12.72	11.66	9.01	853	68.3
14.	L-Shape	11.13	12.99	11.66	11.66	11.13	11.13	1054	84.3
15.	Screw Pattern	9.01	12.99	12.72	12.19	11.66	9.01	853	68.3

minimize these issues. The performance of various array configurations under different types of shading patterns is given in the tables from Table 3 to Table 13 and the same depicted in Figures 24 to Figure 29.

The PV array configurations are classified into various categories like poor, average, consistent, best based on the power generation and the shade dispersion capability. This classification gives the overall view about the performance of each array configurations.

Table 14 shows the different configurations of arrays that were tested, along with their performance in different shading conditions.. The configurations tested were Series, Parallel, Series-Parallel, TCT, SuDoKu, Futoshiki, Magic Square, Com. Square, SD-PAR, Odd-Even, Chaotic Map, Dom. Square, Sky Crapper, L-Shape, and Screw Pattern. The 11Rank'' column indicates the overall ranking of each configuration based on its performance in the experiment. The configurations with the best performance were Parallel, SD-PAR, Odd-Even, Chaotic Map, Dom. Square, L-Shape, and Screw Pattern, all of which received a ranking of ''Best.'' The Series configuration performed the worst, receiving a ranking of ''Poor.''

VII. EXPERIMENTAL VALIDATION OF SELECTED ARRAY CONFIGURATIONS

From the simulation results, the Magic square array configuration is performing consistent in all kinds of shading patterns. The DmSq, SyC, L-Shape and Screw are also performing well, but in some kind of shading patterns, they failed to disperse the shading. But in most of the cases

TABLE 11. Performance of various array configurations under SW shading pattern.

S.No	Array Configuration	Row Current, I_{ROW} (A)					Short Circuit Current, I_{SC} (A)	Maximum Power Output, P_M (W)	Efficiency, η (%)
		I_{R1}	I_{R1}	I_{R1}	I_{R1}	I_{R1}			
1.	Series	0.53	-	-	-	-	0.53	251	20.1
2.	Parallel	56.18	-	-	-	-	56.18	1064	85.1
3.	Series-Parallel	0.53	0.53	2.65	2.65	2.65	9.01	853	68.3
4.	TCT	11.66	11.39	10.6	11.93	10.6	10.6	1004	80.3
5.	SuDoKu	11.13	10.87	12.46	11.66	10.07	10.07	954	76.3
6.	Futoshiki	10.6	11.66	12.72	11.13	10.07	10.07	954	76.3
7.	Magic Square	12.46	12.72	12.19	11.13	9.54	9.54	904	72.3
8.	Com. Square	13.25	13.25	8.75	7.69	13.25	7.69	728	58.2
9.	SD-PAR	10.87	12.46	11.66	10.07	11.13	10.01	954	76.3
10.	Odd-Even	12.19	9.54	11.93	10.34	12.19	9.54	904	72.3
11.	Chaotic Map	12.99	13.25	8.22	9.28	13.25	8.22	778	62.2
12.	Dom. Square	11.13	10.07	10.87	12.19	12.93	10.07	954	76.3
13.	Sky Crapper	11.66	10.6	11.93	12.46	9.54	9.54	904	72.3
14.	L-Shape	12.46	12.46	11.66	10.6	9.01	9.01	853	68.3
15.	Screw Pattern	10.6	12.72	12.19	11.13	9.54	9.54	904	72.3

TABLE 12. Performance of various array configurations under LN shading pattern.

S.No	Array Configuration	Row Current, I_{ROW} (A)					Short Circuit Current, I_{SC} (A)	Maximum Power Output, P_M (W)	Efficiency, η (%)
		IR1	IR1	IR1	IR1	IR1			
1.	Series	0.53	-	-	-	-	0.53	251	20.1
2.	Parallel	53	-	-	-	-	53	1004	80.3
3.	Series-Parallel	1.06	0.53	1.59	0.53	2.65	6.36	602	48.2
4.	TCT	9.8	7.69	9.01	13.25	13.25	7.69	728	58.2
5.	SuDoKu	9.01	11.4	12.46	10.07	10.07	9.01	853	68.3
6.	Futoshiki	9.01	10.07	12.46	12.34	11.13	9.01	853	68.3
7.	Magic Square	11.4	10.34	11.66	12.19	10.87	10.34	979	78.3
8.	Com. Square	9.28	13.25	10.87	9.01	10.6	9.01	853	68.3
9.	SD-PAR	11.4	12.46	10.07	10.07	9.01	9.01	853	68.3
10.	Odd-Even	9.54	11.13	10.34	9.81	12.19	9.54	904	72.3
11.	Chaotic Map	12.99	11.66	7.16	12.99	10.6	7.16	678	54.2
12.	Dom. Square	9.54	10.34	10.6	10.07	12.46	9.54	904	72.3
13.	Sky Crapper	10.6	9.01	11.93	10.6	10.87	9.01	853	68.3
14.	L-Shape	10.6	12.19	10.07	9.54	10.6	9.54	904	72.3
15.	Screw Pattern	10.07	11.93	11.4	10.07	9.54	9.54	904	72.3

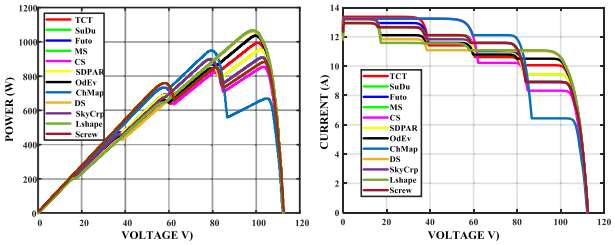

FIGURE 25. Characteristic curves of PV array configurations under Random shading pattern.

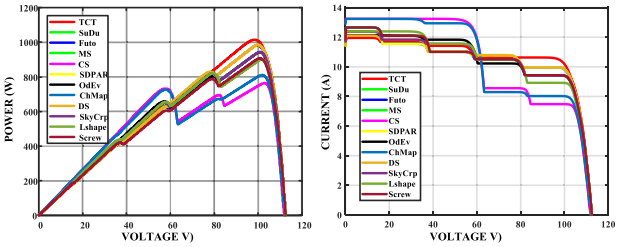

FIGURE 26. Characteristic curves of PV array configurations under SN shading pattern.

they are performing well. So that, these five configurations are analyzed in the real-time environment. The validations has been carried out in 5 × 5 PV array with different types of PV modules such as mono-crystalline PV and poly-crystalline PV. In this experiment, the performance of a 5 × 5 photovoltaic (PV) array is validated. It is important to note that the physical structure of the PV panels belonged to a 10 × 3 array. However, due to the panels being permanently

TABLE 13. Performance of various array configurations under LW shading pattern.

S. No	Array Configuration	Row Current, I_{ROW} (A)					Short Circuit Current, I_{SC} (A)	Maximum Power Output, P_M (W)	Efficiency, η (%)
		I_{R1}	I_{R1}	I_{R1}	I_{R1}	I_{R1}			
1.	Series	0.53	-	-	-	-	0.53	251	20.1
2.	Parallel	48.2	-	-	-	-	48.2	914	73.1
3.	Series-Parallel	0.53	1.06	0.53	0.53	2.65	5.3	502	40.2
4.	TCT	8.48	7.16	9.81	9.54	13.25	7.16	678	54.2
5.	SuDoKu	7.42	10.1	9.81	11.4	9.54	7.42	703	56.2
6.	Futoshiki	7.95	11.4	8.48	9.28	11.67	7.95	753	60.2
7.	Magic Square	9.01	7.95	9.28	10.6	9.01	7.95	753	60.2
8.	Com. Square	8.22	13.25	9.28	9.54	7.95	7.95	753	60.2
9.	SD-PAR	10.07	9.81	11.4	9.54	7.42	7.42	703	56.2
10.	Odd-Even	9.28	11.66	7.69	9.54	10.07	7.69	728	58.2
11.	Chaotic Map	10.1	10.6	7.69	9.01	7.95	7.69	728	58.2
12.	Dom. Square	10.34	7.95	10.34	10.6	9.01	7.95	753	60.2
13.	Sky Crapper	10.6	9.54	7.42	11.66	9.01	7.42	703	56.2
14.	L-Shape	7.01	7.42	11.66	10.07	10.07	7.42	703	56.2
15.	Screw Pattern	10.07	9.01	8.75	10.34	10.07	8.75	828	66.3

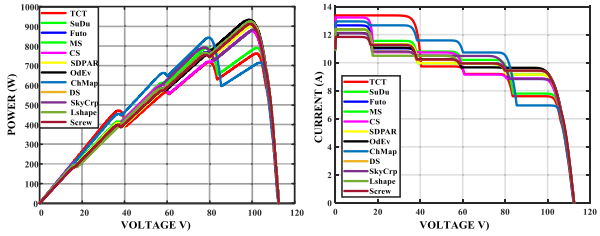

FIGURE 27. Characteristic curves of PV array configurations under SW shading pattern.

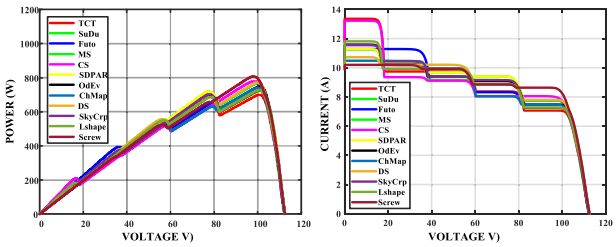

FIGURE 28. Characteristic curves of PV array configurations under LN shading pattern.

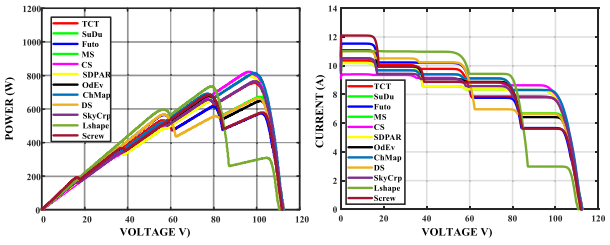

FIGURE 29. Characteristic curves of PV array configurations under LW shading pattern.

TABLE 14. Classification of each array configuraitons.

S.No	Array Configuration	First Five	Second Five	Third Five	Rank
1.	Series	-	-	10	Poor
2.	Parallel	10	-	-	Best
3.	Series-Parallel	-	3	7	Average
4.	TCT	2	2	6	Average
5.	SuDoKu	6	4	-	Average
6.	Futoshiki	5	5	-	Average
7.	Magic Square	9	1	-	Consistent
8.	Com. Square	5	5	-	Average
9.	SD-PAR	8	2	-	Best
10.	Odd-Even	8	2	-	Best
11.	Chaotic Map	8	2	-	Best
12.	Dom. Square	8	2	-	Best
13.	Sky Crapper	7	3		Average
14.	L-Shape	9	1	-	Best
15.	Screw Pattern	8	2	-	Best

TABLE 15. Electrical characteristics of PV panel.

S.No	Parameters	Ratings	Units	Type
1.	Power (P_{max})	270	W	Mono-crystalline
2.	Open Circuit Voltage (V_{OC})	38.20	V	
3.	Short Circuit Current (I_{SC})	9.19	A	
4.	Voltage at Maximum Power (V_{pm})	31.10	V	
5.	Current at Maximum Power (I_{pm})	8.67	A	
6.	Power (P_{max})	270	W	Poly-crystalline
7.	Open Circuit Voltage (V_{OC})	38.04	V	
8.	Short Circuit Current (I_{SC})	8.56	A	
9.	Voltage at Maximum Power (V_{pm})	30.43	V	
10.	Current at Maximum Power (I_{pm})	8.22	A	

mounted on the clamps, it restricts to physically change the arrangement to represent a 5 × 5 PV array in the experiment. The specifications of the PV modules used for the hardware setup is given in table 14. In twenty five PV modules, eighteen

FIGURE 30. Photograph of the experimental setup.

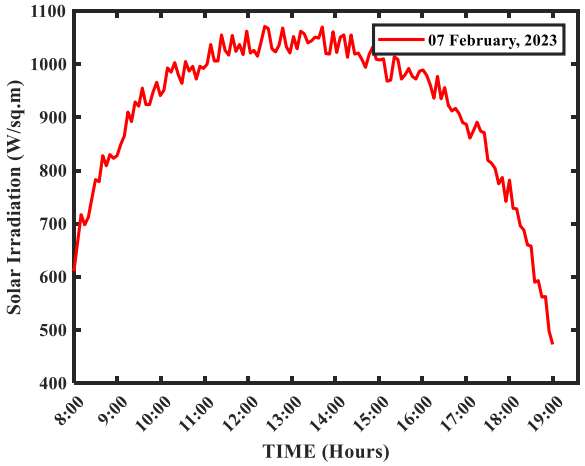

FIGURE 31. Solar Irradiation on 07 February 2023.

FIGURE 32. Fault creation on PV panels.

poly crystalline PV modules and seven mono-crystalline PV modules are used. Along with the partial shading some other factors like aging of PV modules, replaced PV modules with different specifications, uneven current ratings are influencing on the mismatch losses. Figure 30 shows the PV array structure for the experimental validation. In some of the PV modules.

Different types of PV materials with different specification are connected as a PV array. The individual terminals of the

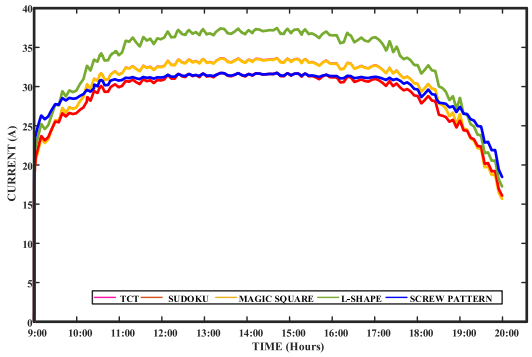

FIGURE 33. Current output from each configurations 50% of shading.

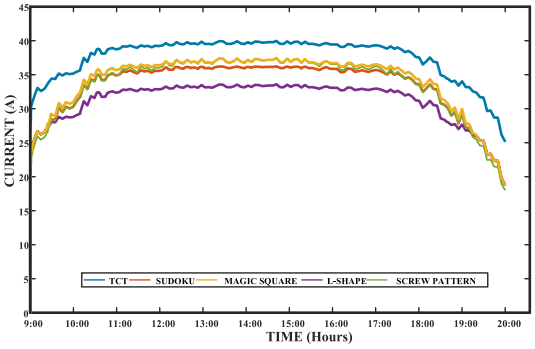

FIGURE 34. Current output from each configurations 30% of shading.

PV array is been connected in junction box, at where the configuration can be interchanged. The shadings and faults are been created in the PV array as shown in figure 31. Dust particles are accumulated on the PV surface, also sheets covered on the PV surface to create the partial shading. The experimental validation is carried out on 07th February, 2023. The irradiation data on this day is plotted as a graph as shown in figure 32. Two different kind of shading patterns are created on the panel surface. In the first shading pattern, 50% of the PV surface was covered. In this shading conditions, L-shape configuration generates maximum current all the day. The magic square configuration method has the second highest power generation and TCT, SuDoku, Screw pattern configuration generating nearly same power. In this shading condition, the L-shape has the best shade dispersion level as compared to other configurations.

In second case, 25% of the PV surface has been covered with the sheets. In this condition, TCT configuration has the best power generation among all other array configurations. The L-Shape configurations which has highest power generation in the previous case, has the least power generation in this case. Whereas magic square configuration has generates second highest power in this case. The other configuration has generates power next to MS configuration. The irradiation data and current generation from PV has been measured for every five minutes interval. PV data logger constructed using Arduino controller is used for measuring the voltage and current and a Lux meter is used for measuring the solar

irradiation level. The measured data of irradiation, current for the entire day of 07th February, 2023 is plotted as graphs as shown in figure 31, figure 32 and figure 33.

VIII. CONCLUSION

This work analyzed and validated various PV array configurations using MATLAB/Simulink® and experimental validation. The work found that the magic square puzzle pattern array configuration consistently performed well under different shading patterns, with an average efficiency of 74.3%. also, it ranked the efficiency of other array configurations based on short circuit current and power generation. The results show that by dispersing shading uniformly over the PV array, mismatch losses can be minimized, resulting in increased power output. The TCT and magic square array configurations were found to be effective solutions to partial shading, with the magic square configuration showing a significant improvement in power generation efficiency compared to the series configuration. The experimental validation confirmed the simulation results and provided additional insights into the performance of the array configurations under different environmental conditions. In conclusion, this work provides valuable insights into the performance of various PV array configurations and identifies effective solutions to partial shading. The study's results can guide the selection of an appropriate PV array configuration for a specific environmental condition and inform future research on enhancing PV array efficiency.

REFERENCES

[1] S. Serna-Garcés, J. Bastidas-Rodríguez, and C. Ramos-Paja, "Reconfiguration of urban photovoltaic arrays using commercial devices," *Energies*, vol. 9, no. 1, p. 2, Dec. 2015.

[2] S. K. Kar, A. Sharma, and B. Roy, "Solar energy market developments in India," *Renew. Sustain. Energy Rev.*, vol. 62, pp. 121–133, Sep. 2016, doi: 10.1016/j.rser.2016.04.043.

[3] B. Parida, S. Iniyan, and R. Goic, "A review of solar photovoltaic technologies," *Renew. Sustain. Energy Rev.*, vol. 15, no. 3, pp. 1625–1636, Apr. 2011, doi: 10.1016/j.rser.2010.11.032.

[4] W. Palz, "Role of new and renewable energies in future energy systems," *Int. J. Sol. Energy*, vol. 14, no. 3, pp. 127–140, Jan. 1994, doi: 10.1080/01425919408909805.

[5] K. Lappalainen and S. Valkealahti, "Effects of irradiance transition characteristics on the mismatch losses of different electrical PV array configurations," *IET Renew. Power Gener.*, vol. 11, no. 2, pp. 248–254, Feb. 2017.

[6] K. Lappalainen and S. Valkealahti, "Photovoltaic mismatch losses caused by moving clouds," *Sol. Energy*, vol. 158, pp. 455–461, Dec. 2017.

[7] A. Woyte, J. Nijs, and R. Belmans, "Partial shadowing of photovoltaic arrays with different system configurations: Literature review and field test results," *Sol. Energy*, vol. 74, no. 3, pp. 217–233, Mar. 2003.

[8] E. I. Batzelis, P. S. Georgilakis, and S. A. Papathanassiou, "Energy models for photovoltaic systems under partial shading conditions: A comprehensive review," *IET Renew. Power Gener.*, vol. 9, no. 4, pp. 340–349, May 2015.

[9] J. Bai, Y. Cao, Y. Hao, Z. Zhang, S. Liu, and F. Cao, "Characteristic output of PV systems under partial shading or mismatch conditions," *Sol. Energy*, vol. 112, pp. 41–54, Feb. 2015.

[10] A. Gupta and Y. K. Chauhan, "Detailed performance analysis of realistic solar photovoltaic systems at extensive climatic conditions," *Energy*, vol. 116, pp. 716–734, Dec. 2016.

[11] I. Drouiche, S. Harrouni, and A. H. Arab, "A new approach for modelling the aging PV module upon experimental I–V curves by combining translation method and five-parameters model," *Electr. Power Syst. Res.*, vol. 163, pp. 231–241, Oct. 2018.

[12] Y. Yang, D. Zhang, and A. Li, "Layout optimization of spacecraft-based solar array under partially shaded conditions," *Sol. Energy*, vol. 167, pp. 84–94, Jun. 2018.

[13] S. Gallardo-Saavedra and B. Karlsson, "Simulation, validation and analysis of shading effects on a PV system," *Sol. Energy*, vol. 170, pp. 828–839, Aug. 2018.

[14] E. I. Batzelis, S. A. Papathanassiou, and B. C. Pal, "PV system control to provide active power reserves under partial shading conditions," *IEEE Trans. Power Electron.*, vol. 33, no. 11, pp. 9163–9175, Nov. 2018.

[15] F. Bayrak, G. Ertürk, and H. F. Oztop, "Effects of partial shading on energy and exergy efficiencies for photovoltaic panels," *J. Cleaner Prod.*, vol. 164, pp. 58–69, Oct. 2017.

[16] T. Hong, C. Koo, J. Oh, and K. Jeong, "Nonlinearity analysis of the shading effect on the technical-economic performance of the building-integrated photovoltaic blind," *Appl. Energy*, vol. 194, pp. 467–480, May 2017.

[17] M. M. Escribano, M. G. Solano, I. D. P. L. Laita, J. M. Alvarez, L. Marroyo, and E. L. Pigueiras, "Module temperature dispersion within a large PV array: Observations at the Amareleja PV Pplant," *IEEE J. Photovolt.*, vol. 8, no. 6, pp. 1725–1731, Nov. 2018.

[18] A. Dhoke, R. Sharma, and T. K. Saha, "PV module degradation analysis and impact on settings of overcurrent protection devices," *Sol. Energy*, vol. 160, pp. 360–367, Jan. 2018.

[19] V. Sharma and S. S. Chandel, "A novel study for determining early life degradation of multi-crystalline-silicon photovoltaic modules observed in western Himalayan Indian climatic conditions," *Sol. Energy*, vol. 134, pp. 32–44, Sep. 2016.

[20] M. A. M. Ramli, E. Prasetyono, R. W. Wicaksana, N. A. Windarko, K. Sedraoui, and Y. A. Al-Turki, "On the investigation of photovoltaic output power reduction due to dust accumulation and weather conditions," *Renew. Energy*, vol. 99, pp. 836–844, Dec. 2016.

[21] A. Gholami, I. Khazaee, S. Eslami, M. Zandi, and E. Akrami, "Experimental investigation of dust deposition effects on photo-voltaic output performance," *Sol. Energy*, vol. 159, pp. 346–352, Jan. 2018.

[22] F. M. Zaihidee, S. Mekhilef, M. Seyedmahmoudian, and B. Horan, "Dust as an unalterable deteriorative factor affecting PV panel's efficiency: Why and how," *Renew. Sustain. Energy Rev.*, vol. 65, pp. 1267–1278, Nov. 2016.

[23] E. Díaz-Dorado, J. Cidrás, and C. Carrillo, "Discretized model for partially shaded PV arrays composed of PV panels with overlapping bypass diodes," *Sol. Energy*, vol. 157, pp. 103–115, Nov. 2017.

[24] C. Greacen and D. Green, "The role of bypass diodes in the failure of solar battery charging stations in Thailand," *Sol. Energy Mater. Sol. Cells*, vol. 70, no. 2, pp. 141–149, Dec. 2001.

[25] S. W. Ko, Y. C. Ju, H. M. Hwang, J. H. So, Y.-S. Jung, H.-J. Song, H.-E. Song, S.-H. Kim, and G. H. Kang, "Electric and thermal characteristics of photovoltaic modules under partial shading and with a damaged bypass diode," *Energy*, vol. 128, pp. 232–243, Jun. 2017.

[26] S. Silvestre, A. Boronat, and A. Chouder, "Study of bypass diodes configuration on PV modules," *Appl. Energy*, vol. 86, no. 9, pp. 1632–1640, Sep. 2009.

[27] H. Zheng, S. Li, R. Challoo, and J. Proano, "Shading and bypass diode impacts to energy extraction of PV arrays under different converter configurations," *Renew. Energy*, vol. 68, pp. 58–66, Aug. 2014.

[28] S. Vemuru, P. Singh, and M. Niamat, "Modeling impact of bypass diodes on photovoltaic cell performance under partial shading," in *Proc. IEEE Int. Conf. Electro/Inf. Technol.*, May 2012, pp. 1–5.

[29] H. Ziar, S. Mansourpour, E. Afjei, and M. Kazemi, "Bypass diode characteristic effect on the behavior of solar PV array at shadow condition," in *Proc. 3rd Power Electron. Drive Syst. Technol. (PEDSTC)*, Feb. 2012, pp. 229–233.

[30] S. Daliento, F. D. Napoli, P. Guerriero, and V. d'Alessandro, "A modified bypass circuit for improved hot spot reliability of solar panels subject to partial shading," *Sol. Energy*, vol. 134, pp. 211–218, Sep. 2016.

[31] H. Ziar, M. Nouri, B. Asaei, and S. Farhangi, "Analysis of overcurrent occurrence in photovoltaic modules with overlapped by-pass diodes at partial shading," *IEEE J. Photovolt.*, vol. 4, no. 2, pp. 713–721, Mar. 2014.

[32] V. Quaschning and R. Hanitsch, "Numerical simulation of current-voltage characteristics of photovoltaic systems with shaded solar cells," *Sol. Energy*, vol. 56, no. 6, pp. 513–520, Jun. 1996.

[33] M. Alonsogarcia, J. Ruiz, and F. Chenlo, "Experimental study of mismatch and shading effects in the—Characteristic of a photovoltaic module," *Sol. Energy Mater. Sol. Cells*, vol. 90, no. 3, pp. 329–340, Feb. 2006.

[34] E. Díaz-Dorado, J. Cidrás, and C. Carrillo, "Discrete I–V model for partially shaded PV-arrays," *Sol. Energy*, vol. 103, pp. 96–107, May 2014.

[35] F. Belhachat and C. Larbes, "Global maximum power point tracking based on ANFIS approach for PV array configurations under partial shading conditions," *Renew. Sustain. Energy Rev.*, vol. 77, pp. 875–889, Sep. 2017.

[36] V. V. Ramana, A. Mudlapur, R. V. Damodaran, B. Venkatesaperumal, and S. Mishra, "Global peak tracking of photovoltaic array under mismatching conditions using current control," *IEEE Trans. Energy Convers.*, vol. 34, no. 1, pp. 313–320, Mar. 2019.

[37] H. S. Sahu and S. K. Nayak, "Estimation of maximum power point of a double diode model photovoltaic module," *IET Power Electron.*, vol. 10, no. 6, pp. 667–675, May 2017.

[38] Y. E. Abu Eldahab, N. H. Saad, and A. Zekry, "Enhancing the tracking techniques for the global maximum power point under partial shading conditions," *Renew. Sustain. Energy Rev.*, vol. 73, pp. 1173–1183, Jun. 2017.

[39] A. Murtaza, M. Chiaberge, F. Spertino, D. Boero, and M. D. Giuseppe, "A maximum power point tracking technique based on bypass diode mechanism for PV arrays under partial shading," *Energy Buildings*, vol. 73, pp. 13–25, Apr. 2014.

[40] G. Li, Y. Jin, M. W. Akram, X. Chen, and J. Ji, "Application of bio-inspired algorithms in maximum power point tracking for PV systems under partial shading conditions—A review," *Renew. Sustain. Energy Rev.*, vol. 81, pp. 840–873, Jan. 2018.

[41] M. L. Orozco-Gutierrez, G. Petrone, J. M. Ramirez-Scarpetta, G. Spagnuolo, and C. A. Ramos-Paja, "A method for the fast estimation of the maximum power points in mismatched PV strings," *Electr. Power Syst. Res.*, vol. 121, pp. 115–125, Apr. 2015.

[42] A. Ashouri-Zadeh, M. Toulabi, A. S. Dobakhshari, S. Taghipour-Broujeni, and A. M. Ranjbar, "A novel technique to extract the maximum power of photovoltaic array in partial shading conditions," *Int. J. Electr. Power Energy Syst.*, vol. 101, pp. 500–512, Oct. 2018.

[43] G. Dileep and S. N. Singh, "Application of soft computing techniques for maximum power point tracking of SPV system," *Solar Energy*, vol. 141, pp. 182–202, Jan. 2017.

[44] K. Kaced, C. Larbes, N. Ramzan, M. Bounabi, and Z. E. Dahmane, "Bat algorithm based maximum power point tracking for photovoltaic system under partial shading conditions," *Sol. Energy*, vol. 158, pp. 490–503, Dec. 2017.

[45] J. P. Ram and N. Rajasekar, "A novel flower pollination based global maximum power point method for solar maximum power point tracking," *IEEE Trans. Power Electron.*, vol. 32, no. 11, pp. 8486–8499, Nov. 2017.

[46] F. Belhachat and C. Larbes, "A review of global maximum power point tracking techniques of photovoltaic system under partial shading conditions," *Renew. Sustain. Energy Rev.*, vol. 92, pp. 513–553, Sep. 2018.

[47] S. R. Pendem and S. Mikkili, "Modeling, simulation and performance analysis of solar PV array configurations (series, series–parallel and honey-comb) to extract maximum power under partial shading conditions," *Energy Rep.*, vol. 4, pp. 274–287, Nov. 2018.

[48] S. Mohammadnejad, A. Khalafi, and S. M. Ahmadi, "Mathematical analysis of total-cross-tied photovoltaic array under partial shading condition and its comparison with other configurations," *Sol. Energy*, vol. 133, pp. 501–511, Aug. 2016.

[49] F. Belhachat and C. Larbes, "Modeling, analysis and comparison of solar photovoltaic array configurations under partial shading conditions," *Sol. Energy*, vol. 120, pp. 399–418, Oct. 2015.

[50] K. Lappalainen and S. Valkealahti, "Effects of PV array layout, electrical configuration and geographic orientation on mismatch losses caused by moving clouds," *Sol. Energy*, vol. 144, pp. 548–555, Mar. 2017.

[51] D. P. Winston, S. Kumaravel, B. P. Kumar, and S. Devakirubakaran, "Performance improvement of solar PV array topologies during various partial shading conditions," *Sol. Energy*, vol. 196, pp. 228–242, Jan. 2020.

[52] M. Horoufiany and R. Ghandehari, "Optimization of the sudoku based reconfiguration technique for PV arrays power enhancement under mutual shading conditions," *Sol. Energy*, vol. 159, pp. 1037–1046, Jan. 2018.

[53] B. I. Rani, G. S. Ilango, and C. Nagamani, "Enhanced power generation from PV array under partial shading conditions by shade dispersion using Su Do Ku configuration," *IEEE Trans. Sustain. Energy*, vol. 4, no. 3, pp. 594–601, Jul. 2013.

[54] S. Vijayalekshmy, G. R. Bindu, and S. R. Iyer, "Analysis of various photovoltaic array configurations under shade dispersion by Su Do Ku arrangement during passing cloud conditions," *Indian J. Sci. Technol.*, vol. 8, no. 35, pp. 1–7, Dec. 2015.

[55] H. S. Sahu, S. K. Nayak, and S. Mishra, "Maximizing the power generation of a partially shaded PV array," *IEEE J. Emerg. Sel. Topics Power Electron.*, vol. 4, no. 2, pp. 626–637, Jun. 2016.

[56] S. M. Samikannu, R. Namani, and S. K. Subramaniam, "Power enhancement of partially shaded PV arrays through shade dispersion using magic square configuration," *J. Renew. Sustain. Energy*, vol. 8, no. 6, Nov. 2016, Art. no. 063503.

[57] B. Dhanalakshmi and N. Rajasekar, "A novel competence square based PV array reconfiguration technique for solar PV maximum power extraction," *Energy Convers. Manage.*, vol. 174, pp. 897–912, Oct. 2018.

[58] A. S. Yadav, R. K. Pachauri, Y. K. Chauhan, S. Choudhury, and R. Singh, "Performance enhancement of partially shaded PV array using novel shade dispersion effect on magic-square puzzle configuration," *Sol. Energy*, vol. 144, pp. 780–797, Mar. 2017.

[59] P. R. Satpathy, R. Sharma, and S. Dash, "An efficient SD-PAR technique for maximum power generation from modules of partially shaded PV arrays," *Energy*, vol. 175, pp. 182–194, May 2019.

[60] I. Nasiruddin, S. Khatoon, M. F. Jalil, and R. C. Bansal, "Shade diffusion of partial shaded PV array by using odd-even structure," *Sol. Energy*, vol. 181, pp. 519–529, Mar. 2019.

[61] V. M. R. Tatabhatla, A. Agarwal, and T. Kanumuri, "Improved power generation by dispersing the uniform and non-uniform partial shades in solar photovoltaic array," *Energy Convers. Manage.*, vol. 197, Oct. 2019, Art. no. 111825.

[62] S. Devakirubakaran and C. Bharatiraja, "A novel fused fibonacci-geometric number pattern-based PV array configuration for mitigating the mismatch losses," in *Proc. IEEE IAS Global Conf. Renew. Energy Hydrogen Technol. (GlobConHT)*, Mar. 2023, pp. 1–6, doi: 10.1109/GlobConHT56829.2023.10087573.

[63] S. Alwar, D. Samithas, M. S. Boominathan, P. K. Balachandran, and L. Mihet-Popa, "Performance analysis of thermal image processing-based photovoltaic fault detection and PV array reconfiguration—A detailed experimentation," *Energies*, vol. 15, no. 22, p. 8450, Nov. 2022, doi: 10.3390/en15228450.

[64] B. Dhanalakshmi and N. Rajasekar, "Dominance square based array reconfiguration scheme for power loss reduction in solar Photo-Voltaic (PV) systems," *Energy Convers. Manage.*, vol. 156, pp. 84–102, Jan. 2018.

[65] M. S. S. Nihanth, J. P. Ram, D. S. Pillai, A. M. Y. M. Ghias, A. Garg, and N. Rajasekar, "Enhanced power production in PV arrays using a new skyscraper puzzle based one-time reconfiguration procedure under partial shade conditions (PSCs)," *Sol. Energy*, vol. 194, pp. 209–224, Dec. 2019.

[66] A. Srinivasan, S. Devakirubakaran, B. M. Sundaram, P. K. Balachandran, S. K. Cherukuri, D. P. Winston, T. S. Babu, and H. H. Alhelou, "L-shape propagated array configuration with dynamic reconfiguration algorithm for enhancing energy conversion rate of partial shaded photovoltaic systems," *IEEE Access*, vol. 9, pp. 97661–97674, 2021.

[67] B. P. Kumar, S. K. Cherukuri, K. R. Kaniganti, N. Karuppiah, R. Muniraj, T. S. Babu, and H. H. Alhelou, "Performance enhancement of partial shaded photovoltaic system with the novel screw pattern array configuration scheme," *IEEE Access*, vol. 10, pp. 1731–1744, 2022.

[68] K. Lappalainen and S. Valkealahti, "Output power variation of different PV array configurations during irradiance transitions caused by moving clouds," *Appl. Energy*, vol. 190, pp. 902–910, Mar. 2017.

[69] S. R. Pendem and S. Mikkili, "Modelling and performance assessment of PV array topologies under partial shading conditions to mitigate the mismatching power losses," *Sol. Energy*, vol. 160, pp. 303–321, Jan. 2018.

[70] H. S. Sahu and S. K. Nayak, "Power enhancement of partially shaded PV array by using a novel approach for shade dispersion," in *Proc. IEEE Innov. Smart Grid Technol. Asia (ISGT ASIA)*, May 2014, pp. 498–503.

[71] O. Bingöl and B. Özkaya, "Analysis and comparison of different PV array configurations under partial shading conditions," *Sol. Energy*, vol. 160, pp. 336–343, Jan. 2018.

[72] A. S. Yadav, R. K. Pachauri, and Y. K. Chauhan, "Comprehensive investigation of PV arrays with puzzle shade dispersion for improved performance," *Sol. Energy*, vol. 129, pp. 256–285, May 2016.

[73] X. Qing, H. Sun, X. Feng, and C. Y. Chung, "Submodule-based modeling and simulation of a series-parallel photovoltaic array under mismatch conditions," *IEEE J. Photovolt.*, vol. 7, no. 6, pp. 1731–1739, Nov. 2017.

[74] S. Malathy and R. Ramaprabha, "A static PV array architecture to enhance power generation under partial shaded conditions," in *Proc. IEEE 11th Int. Conf. Power Electron. Drive Syst.*, Jun. 2015, pp. 341–346.

[75] Y.-J. Wang and P.-C. Hsu, "An investigation on partial shading of PV modules with different connection configurations of PV cells," *Energy*, vol. 36, no. 5, pp. 3069–3078, May 2011.

[76] G. Madhusudanan, S. Senthilkumar, I. Anand, and P. Sanjeevikumar, "A shade dispersion scheme using Latin square arrangement to enhance power production in solar photovoltaic array under partial shading conditions," *J. Renew. Sustain. Energy*, vol. 10, no. 5, Sep. 2018, Art. no. 053506.

[77] M. L. Orozco-Gutierrez, G. Spagnuolo, J. M. Ramirez-Scarpetta, G. Petrone, and C. A. Ramos-Paja, "Optimized configuration of mismatched photovoltaic arrays," *IEEE J. Photovolt.*, vol. 6, no. 5, pp. 1210–1220, Sep. 2016.

[78] P. Srinivasa Rao, P. Dinesh, G. Saravana Ilango, and C. Nagamani, "Optimal Su-Do-Ku based interconnection scheme for increased power output from PV array under partial shading conditions," *Frontiers Energy*, vol. 9, no. 2, pp. 199–210, Jun. 2015.

[79] S. R. Potnuru, D. Pattabiraman, S. I. Ganesan, and N. Chilakapati, "Positioning of PV panels for reduction in line losses and mismatch losses in PV array," *Renew. Energy*, vol. 78, pp. 264–275, Jun. 2015.

[80] P. Srinivasa Rao, G. Saravana Ilango, and C. Nagamani, "Maximum power from PV arrays using a fixed configuration under different shading conditions," *IEEE J. Photovolt.*, vol. 4, no. 2, pp. 679–686, Mar. 2014.

[81] J. P. Storey, P. R. Wilson, and D. Bagnall, "Improved optimization strategy for irradiance equalization in dynamic photovoltaic arrays," *IEEE Trans. Power Electron.*, vol. 28, no. 6, pp. 2946–2956, Jun. 2013.

[82] G. Velasco-Quesada, J. J. Negroni, F. Guinjoan, and R. Pique, "Irradiance equalization method for output power optimization in plant-oriented grid connected PV generators," in *Proc. Eur. Conf. Power Electron. Appl.*, Sep. 2005, p. 10.

[83] S. Vijayalekshmy, G. R. Bindu, and S. Rama Iyer, "A novel Zig–Zag scheme for power enhancement of partially shaded solar arrays," *Sol. Energy*, vol. 135, pp. 92–102, Oct. 2016.

[84] N. Barth, R. Jovanovic, S. Ahzi, and M. A. Khaleel, "PV panel single and double diode models: Optimization of the parameters and temperature dependence," *Sol. Energy Mater. Sol. Cells*, vol. 148, pp. 87–98, Apr. 2016.

[85] Z. Mao, Z. Sunan, M. Peng, S. Yanlong, and Z. Weiping, "Macro-model of PV module and its application for partial shading analysis," *IET Renew. Power Gener.*, vol. 12, no. 15, pp. 1747–1754, 2018.

[86] S.-X. Lun, S. Wang, G.-H. Yang, and T.-T. Guo, "A new explicit double-diode modeling method based on Lambert W-function for photovoltaic arrays," *Sol. Energy*, vol. 116, pp. 69–82, Jun. 2015.

[87] A. Srinivasan, S. Devakirubakaran, and B. M. Sundaram, "Mitigation of mismatch losses in solar PV system—Two-step reconfiguration approach," *Solar Energy*, vol. 206, pp. 640–654, Sep. 2019.

[88] D. P. Winston, K. Ganesan, P. K. B, D. Samithas, and C. B. Baladhanautham, "Experimental investigation on output power enhancement of partial shaded solar photovoltaic system," *Energy Sources, Recovery, Utilization, Environ. Effects*, pp. 1–17, Jun. 2020.

[89] M. Z. Shams El-Dein, M. Kazerani, and M. M. A. Salama, "Optimal photovoltaic array reconfiguration to reduce partial shading losses," *IEEE Trans. Sustain. Energy*, vol. 4, no. 1, pp. 145–153, Jan. 2013.

[90] R. Venkateswari and N. Rajasekar, "Power enhancement of PV system via physical array reconfiguration based lo shu technique," *Energy Convers. Manage.*, vol. 215, Jul. 2020, Art. no. 112885.

[91] M. Jazayeri, K. Jazayeri, and S. Uysal, "Adaptive photovoltaic array reconfiguration based on real cloud patterns to mitigate effects of non-uniform spatial irradiance profiles," *Sol. Energy*, vol. 155, pp. 506–516, Oct. 2017.

[92] M. Simon and E. L. Meyer, "Detection and analysis of hot-spot formation in solar cells," *Sol. Energy Mater. Sol. Cells*, vol. 94, no. 2, pp. 106–113, Feb. 2010.

[93] M. Orkisz, "Estimating effects of individual PV panel failures on PV array output," *IEEE Trans. Ind. Appl.*, vol. 54, no. 5, pp. 4825–4832, Sep. 2018.

[94] A. Peled and J. Appelbaum, "Minimizing the current mismatch resulting from different locations of solar cells within a PV module by proposing new interconnections," *Sol. Energy*, vol. 135, pp. 840–847, Oct. 2016.

[95] N. N. Castellano, J. A. Gázquez Parra, J. Valls-Guirado, and F. Manzano-Agugliaro, "Optimal displacement of photovoltaic array's rows using a novel shading model," *Appl. Energy*, vol. 144, pp. 1–9, Apr. 2015.

[96] B. Yang, R. Shao, M. Zhang, H. Ye, B. Liu, T. Bao, J. Wang, H. Shu, Y. Ren, and H. Ye, "Socio-inspired democratic political algorithm for optimal PV array reconfiguration to mitigate partial shading," *Sustain. Energy Technol. Assessments*, vol. 48, Dec. 2021, Art. no. 101627, doi: 10.1016/j.seta.2021.101627.

[97] B. Aljafari, P. R. Satpathy, S. B. Thanikanti, and H. H. Alhelou, "A zero switch and sensorless reconfiguration approach for sustainable operation of roof-top photovoltaic system during partial shading," *IET Renew. Power Gener.*, vol. 17, no. 6, pp. 1385–1412, Apr. 2023, doi: 10.1049/rpg2.12683.

[98] S. N. Pappachan, "Hybrid red deer with moth flame optimization for reconfiguration process on partially shaded photovoltaic array," *Energy Sources, Recovery, Utilization, Environ. Effects*, pp. 1–27, Feb. 2022, doi: 10.1080/15567036.2022.2029626.

[99] B. Aljafari, P. R. Satpathy, and S. B. Thanikanti, "Partial shading mitigation in PV arrays through dragonfly algorithm based dynamic reconfiguration, Energy,257,2022, Art. no. 124795, doi: 10.1016/j.energy.2022.124795.

[100] S. Rezazadeh, A. Moradzadeh, S. M. Hashemzadeh, K. Pourhossein, B. Mohammadi-Ivatloo, and S. H. Hosseini, "A novel prime numbers-based PV array reconfiguration solution to produce maximum energy under partial shade conditions," *Sustain. Energy Technol. Assessments*, vol. 47, Oct. 2021, Art. no. 101498, doi: 10.1016/j.seta.2021.101498.

[101] P. R. Satpathy, B. Aljafari, and S. B. Thanikanti, "Power losses mitigation through electrical reconfiguration in partial shading prone solar PV arrays," *Optik*, vol. 259, Jun. 2022, Art. no. 168973, doi: 10.1016/j.ijleo.2022.168973.

[102] G. H. K. Varma, V. R. Barry, R. K. Jain, and D. Kumar, "An MMTES algorithm for dynamic photovoltaic array reconfiguration to enhance power output under partial shading conditions," *IET Renew. Power Gener.*, vol. 15, no. 4, pp. 809–820, Mar. 2021, doi: 10.1049/rpg2.12070.

[103] P. R. Satpathy, R. Sharma, and S. Jena, "A shade dispersion interconnection scheme for partially shaded modules in a solar PV array network," *Energy*, vol. 139, pp. 350–365, Nov. 2017, doi: 10.1016/j.energy.2017.07.161.

[104] K. Ms, S. Nattuthurai, B. Chokkalingam, S. Muthusamy, and K. Cherukupalli, "Development of ripple reduced solar photovoltaic regulators using boomerang sliding mode control strategy," *Int. J. Circuit Theory Appl.*, vol. 49, no. 9, pp. 2979–3006, Jun. 2021, doi: 10.1002/cta.3071.

[105] S. B. Thanikanti, B. P. Kumar, S. Devakirubakaran, B. Aljafari, and I. Colak, "A dynamic mismatch loss mitigation algorithm with dual input dual output converter for solar PV systems," *Sol. Energy Mater. Sol. Cells*, vol. 251, Mar. 2023, Art. no. 112163, doi: 10.1016/j.solmat.2022.112163.

S. DEVAKIRUBAKARAN received the B.E. degree in electrical and electronics engineering and the M.E. degree in power systems engineering from Anna University, Chennai, India, in 2014 and 2016, respectively, and the Ph.D. degree from the Department of Science and Technology (DST), Solar Energy Research Initiative (SERI) Scheme Project, in 2022. He is currently a Project Associate with the Center for Electric Mobility, Department of Science and Technology, Government of India, Promotion of University Research and Scientific Excellence (PURSE) Project, SRM Institute of Science and Technology, Chennai. His main research interests include power systems, renewable energy systems, and solar photovoltaic systems.

RAJESH VERMA received the B.E., M.E., and Ph.D. degrees in electronics and communication engineering from the Motilal Nehru National Institute of Technology (MNNIT) Allahabad, Prayagraj, in 1994, 2001, and 2011, respectively. He is currently an Associate Professor with the Department of Electrical Engineering, King Khalid University, Abha, Saudi Arabia.

BHARATIRAJA CHOKKALINGAM (Senior Member, IEEE) received the B.E. degree in electrical and electronics engineering from the Kumaraguru College of Engineering, Coimbatore, India, in 2002, the M.E. degree in power electronics and drives from the Government College of Technology, Coimbatore, in 2006, and the Ph.D. degree from the SRM Institute of Science and Technology, in 2015.

He completed his first Postdoctoral Fellowship with the Centre for Energy and Electric Power, Faculty of Engineering and the Built Environment, Tshwane University of Technology, South Africa, in 2016, with National Research Foundation Funding, and his second Postdoctoral Fellowship with the Department of Electrical and Computer Engineering, Northeastern University, USA. He was a Visiting Research Scientist with Northeastern University, Boston, MA, USA, in 2018, and a Visiting Researcher with the University of South Africa, in 2019 and 2020. He is currently a Professor with the Department of Electrical and Electronics Engineering, SRM Institute of Science and Technology, Kattankulathur Campus, Chennai, India. He is also the Centre Head of the Centre for the E-Mobility, SRM. He is handling/handled government funded projects total worth Rs. 15.65 Cr, including SERB, DST, and TNSCST. He has authored more than 180 research papers and ten books chapters, and ten IPR patents in his name. He also made three Technologies transfers. He is a Senior Member of IEI and IET. He is also a member, mentor, and advisor of many government and private companies bodies. He was a recipient of the DST, Indo-U.S. Bhaskara Advanced Solar Energy, in 2017, and the Young Scientists Fellowship, Tamil Nadu State Council for Science and Technology, in 2018. He was also a recipient of the World's Top 2% Scientists 2021 and 2022 in the Energy category. For more information: https://www.srmist.edu.in/faculty/dr-c-bharatiraja/

LUCIAN MIHET-POPA (Senior Member, IEEE) was born in 1969. He received his Habilitation (2015) and Ph.D. degree (2002) in Electrical Engineering, a Master's degree (2000) in Electric Drives and Power Electronics and a Bachelor's degree (1999) in Electrical Engineering, from the Politehnica University of Timisoara-Romania. Since 2016, he is working as Full Professor in Smart Energy Technology at Oestfold University College in Norway. From 1999 to 2016, Professor Mihet has been with the Politehnica University of Timisoara, Romania. He has also worked as a Research Scientist with the Danish Technical University (2011–2014) and Aalborg University (2000–2002) in Denmark and as a Post Doc with Siegen University in Germany in 2004. Dr. Lucian Mihet has published more than 200 papers in national and international journals and conference proceedings, and 15 books. Since 2017, he has been a Guest Editor of six Special Issues for the MDPI Energies and Applied Sciences Journals, for Maljesi and for the Advances in Meteorology Journal. He has served as Scientific and Technical Programme Committee Member for many IEEE Conferences. Professor Mihet has been granted more than 20 international grants/projects, such as FP7, EEA and Horizon 2020, as well as has been awarded more than 10 national research grants. He is also the Founder and Head of the Research Lab "Intelligent Control of Energy Conversion and Storage Systems" and one of the Coordinators of the Master Program in "Green Energy Technology" at the Faculty of Information Technology, Engineering and Economics. His research interest includes modelling, simulation, control and testing of Energy Conversion Systems, Distributed Energy Resources (DER) components and systems, distributed battery storage systems-DBSS, energy efficiency in smart buildings and smart grids. Professor Mihet was invited to join the Energy and Automotive committees as an Expert by the President and the Honorary President of Atomium European Institute, working in close cooperation with—and under the umbrella—of the EC and EU Parliament, and was Chairing Energy Section of AI4People 2020.